

Thermodynamic Synthesis of Solution Processable Ladder Polymers

Jongbok Lee,¹ Bharath Bangalore Rajeeva,² Tianyu Yuan,^{1,3} Zi-Hao Guo,¹ Yen-Hao Lin,¹

*Mohammed Al-Hashimi,⁴ Yuebing Zheng,² and Lei Fang^{*1,3}*

1. Department of Chemistry, Texas A&M University, 3255 TAMU, College Station, TX, USA

2. Department of Mechanical Engineering, Materials Science and Engineering Program, and Texas Materials Institute, The University of Texas at Austin, Austin, TX, USA

3. Materials Science & Engineering Department, Texas A&M University, 3255 TAMU, College Station, TX, USA

4. Department of Chemistry, Texas A&M University at Qatar, P.O. Box 23874, Doha, Qatar

Supporting Information

*Correspondence Address
Professor Lei Fang Department of Chemistry, Texas A&M University, 3255 TAMU, College Station, TX 77845-3255, USA Tel: +1 (979) 845 3186 E-Mail: fang@chem.tamu.edu

Table of Contents

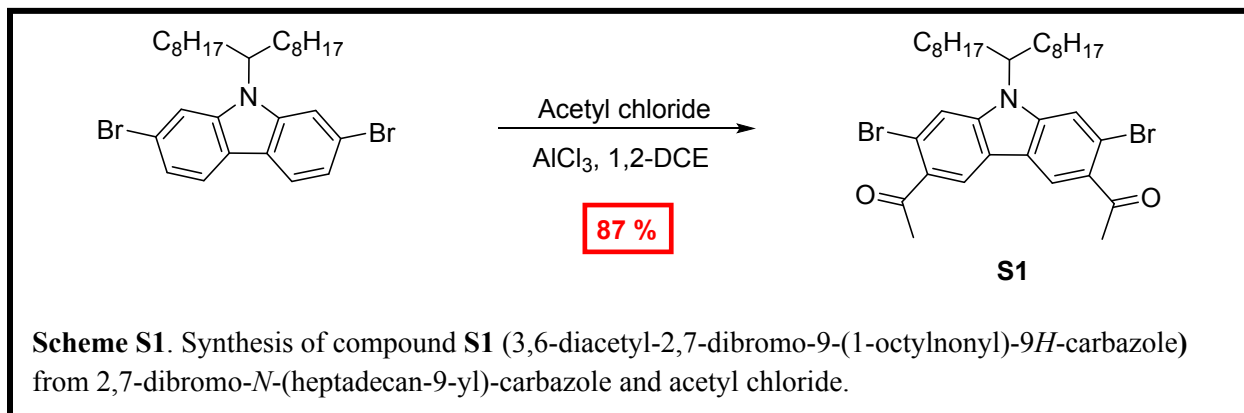
1. General information	2
2. Synthesis	5
3. Synthesis of ¹³C Labeled Compounds	10
4. Ring-closing Olefin Metathesis Optimization.	12
5. Size Exclusion Chromatography (SEC).....	14
6. IR Spectra.....	15
7. ¹H-¹H NOESY Spectrum of 3	17
8. ¹H and ¹³C NMR Spectra	18
9. Quantum Yield.....	29
10. UV/vis and Fluorescence Spectra	30
11. Thermal Gravimetric Analysis (TGA).....	31
12. Differential Scanning Calorimetry (DSC)	32
13. DFT Calculation.....	33
14. Scanning Tunneling Microscopy (STM).....	35
15. X-ray Crystallography	36
16. Reference	37

1. General information

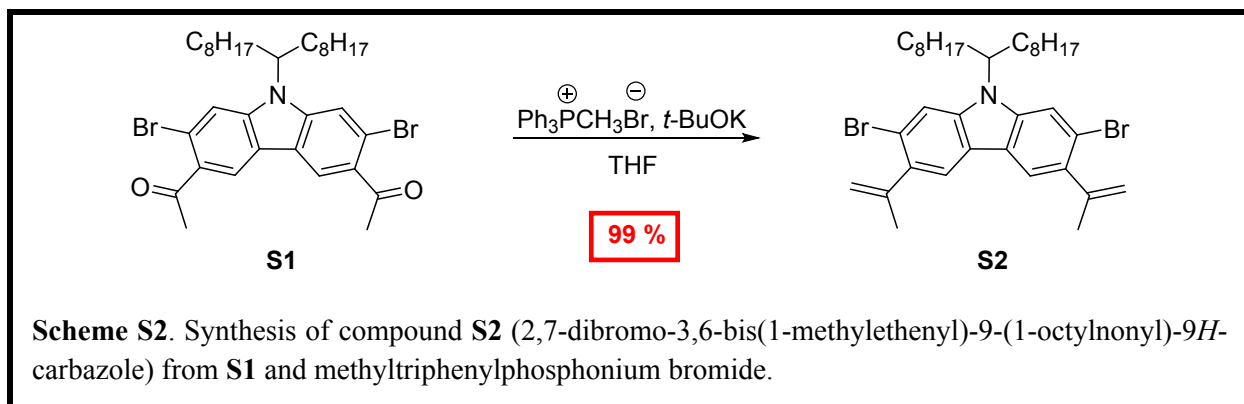
Starting materials and reagents were purchased from Aldrich, Alfa-aesar, and Suna-tech and used as received without further purification. Toluene and THF were dried using IT pure solvent system (PureSolv-MD-5) and used without further treatment. 2,7-Dibromo-*N*-(heptadecan-9-yl)-carbazole¹, 1,4-dibromo-2,5-divinylbenzene², and methyl-¹³C-triphenylphosphonium iodide (99% ¹³C isotope enriched)³ were synthesized according to procedure reported in the literature. Analytical thin-layer chromatography (TLC) was performed on glass that is precoated with silica gel 60-F₂₅₄ (Sorbtech). Flash column chromatography was carried out using Biotage® Isolera™ Prime instrument with various size of SiO₂ Biotage ZIP® cartridge. UV/vis absorption spectra were recorded using Shimadzu UV-2600, while the fluorescent emission spectra were measured on Horiba Fluoromax-4. FT-IR spectra were recorded with ZnSe ATR using Shimadzu IRAffinity-1S. ¹H and ¹³C NMR spectra were obtained on a 500 MHz Varian Inova at room temperature and processed by MestReNova 6.1.0. Chemical shifts are reported in ppm relative to the signals corresponding to the residual non-deuterated solvents (CDCl₃: δ 7.26 for ¹H and 77.16 for ¹³C at room temperature). Size exclusion chromatography (SEC) was performed on TOSOH EcoSEC (HLC-8320GPC) in THF solution at 40°C temperature and the molecular weights calculated using a calibration curve based on polystyrene standards, equipped with TSKgel SuperHM-M and TSKgel SuperH-RC. Preparative SEC was performed in chloroform solution at room temperature using JAI recycling preparative HPLC (LC-92XXII NEXT SERIES). Thermal gravimetric analysis (TGA) was recorded under nitrogen atmosphere with heating rate of 10 °C min⁻¹ from 40 to 900 °C using TA Q500. Differential scanning calorimetry (DSC) was measured on TA Q20 with a heating rate of 10 °C min⁻¹ from 40 to 300 °C. Quantum yields were measured by Edinburgh Instruments FLS920, equipped with integrating sphere

system. High-resolution Matrix-assisted laser desorption/ionization (HR-MALDI) mass spectra were measured on Applied Biosystems 4800 MALDI-TOF. Atomic force microscopy (AFM) images were recorded with Bruker Dimension Icon AFM in a tapping mode and processed using NanoScope Analysis. Optical microscope images were obtained using Olympus BX41 microscope. Grazing-incidence wide-angle X-ray scattering (GIWAXS) measurements were carried out on Sector 8-ID-E at the Advanced Photon Source, Argonne National Laboratory.⁴ Beamline 8-ID-E operates at an energy of 7.35 keV and images were collected from a Pilatus 1MF camera (Dectris), with two exposures for different vertical position of the detector. After flat field correction for detector nonuniformity, the images are combined to fill in the gaps for rows at the borders between modules, leaving dark only the columns of inactive pixels at the center. Using the GIXSGUI package⁵ for Matlab (Mathworks), data are corrected for X-ray polarization, detector sensitivity and geometrical solid-angle. The beam size is 200 μm (h) x 20 μm (v). Sample detector distance is 204 mm. Sample measurement and thermal annealing were carried out under vacuum which is in the range of $2\sim 3 \times 10^{-6}$ bar, with the sample stage interfaced with a Lakeshore 340 unit. Scanning tunneling microscopy (STM) measurement was performed at room temperature using Easyscan 2 system from Nanosurf Inc. The tips were mechanically cut from Pt/Ir wire (80% / 20%, 0.25mm diameter, Nanoscience). Highly ordered pyrolytic graphite (HOPG) substrate purchased from Nanosurf Inc. The STM image was obtained with a tunneling current set point of 0.9 nA and sample bias of 50 mV. X-ray single crystal diffraction measurement was made on a BRUKER APEX 2 X-ray (three-circle) diffractometer. The X-ray radiation employed was generated from a Mo sealed X-ray tube ($K = 0.70173\text{\AA}$ with a potential of 40 kV and a current of 40 mA) fitted with a graphite monochromator in the parallel mode (175 mm collimator with 0.5 mm pinholes).

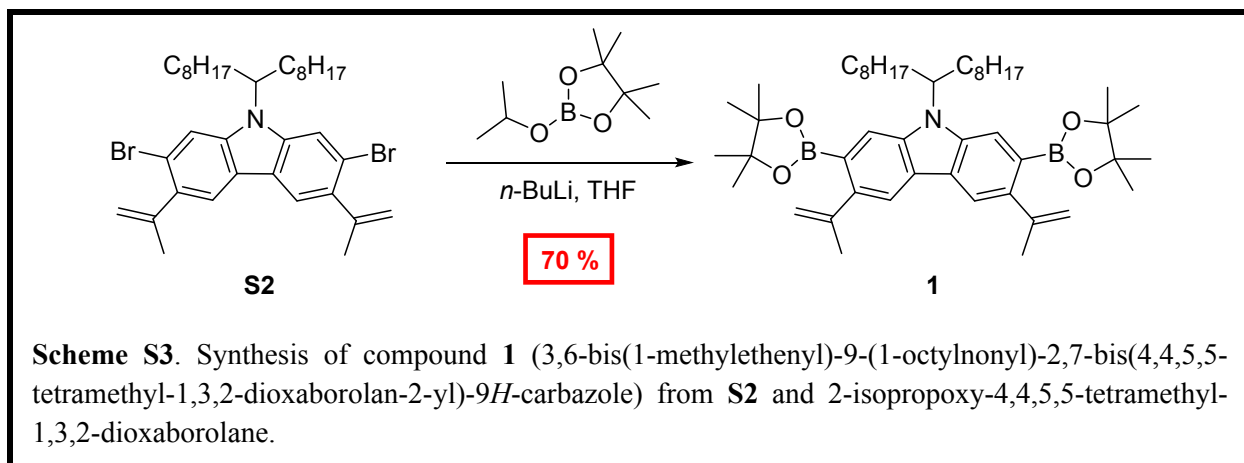
2. Synthesis



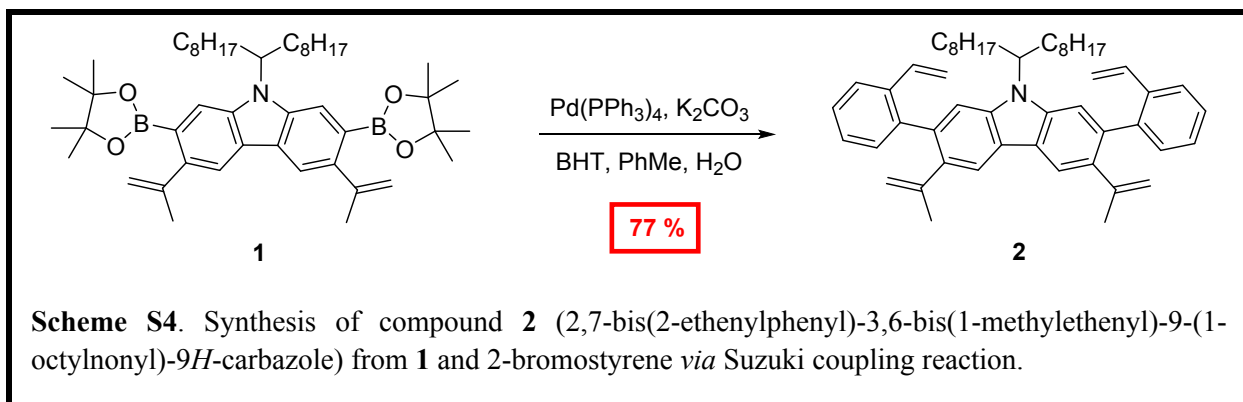
S1 (3,6-diacetyl-2,7-dibromo-9-(1-octylonyl)-9*H*-carbazole): To a mixture of 2,7-dibromo-9-(1-octylonyl)-9*H*-carbazole (4.0 g, 7.1 mmol), AlCl₃ (2.3 g, 17.0 mmol) in 75 mL of anhydrous 1,2-dichloroethane was added acetyl chloride (2.5 mL, 35.5 mmol) slowly under nitrogen atmosphere at room temperature. The reaction mixture was heated to 50 °C with a reflux condenser and stirred for 6 h. The mixture was cooled to 0°C, quenched with ice water, 2*N* HCl, and diluted with DCM. The solution was extracted with CH₂Cl₂ (3 × 30 mL), and the combined organic layer was dried over MgSO₄, filtered through Celite, and concentrated under reduced pressure. The residue was purified by flash column chromatography (SiO₂, hexane/EtOAc 98:2 to 82:18) to give product **S1** (4.0 g, 87%) as a light yellow solid. ¹H NMR (500 MHz, CDCl₃): δ 8.34 (s, 1H), 8.34 (s, 1H), 7.82 (s, 1H), 7.65 (s, 1H), 4.45 (septet, *J* = 5.0 Hz, 1H), 2.77 (s, 6H), 2.19 (m, 2H), 1.93 (m, 2H), 1.18 (m, 22H), 0.95 (m, 2H), 0.82 (t, *J* = 7.0 Hz, 6H). ¹³C NMR (125 MHz, CDCl₃): δ 200.1, 144.5, 141.1, 132.6, 132.5, 122.5, 121.0, 118.2, 117.5, 117.3, 115.1, 57.8, 33.6, 31.8, 30.5, 29.4, 29.2, 26.8, 22.7, 14.2. HR-MALDI: calcd for C₃₃H₄₆Br₂NO₂ [*M*+H]⁺ *m/z* = 648.1876; found *m/z* = 648.1907.



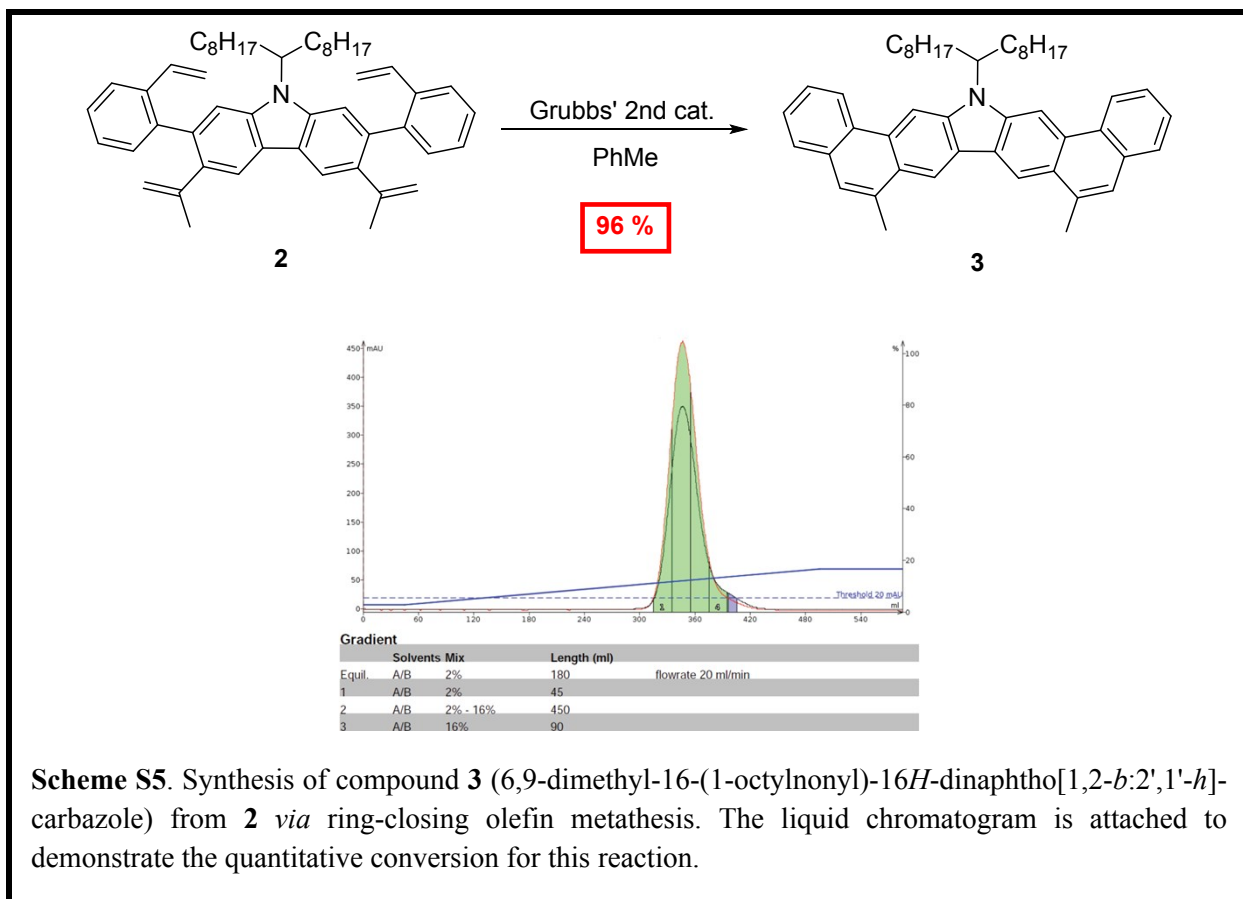
S2 (2,7-dibromo-3,6-bis(1-methylethenyl)-9-(1-octylonyl)-9H-carbazole): To a mixture of methyltriphenylphosphonium bromide (9.4 g, 26.2 mmol) and 100 mL of anhydrous THF was added *t*-BuOK (2.8 g, 24.8 mmol) slowly under nitrogen atmosphere at room temperature. The solution turned light yellow. Compound **S1** (4.0 g, 6.2 mmol) was added into the solution. The mixture was stirred at reflux for 6 h. The reaction mixture was cooled to room temperature and poured into 20 mL of water. THF was removed under reduced pressure, and the residue was extracted with CH₂Cl₂ (3 × 30 mL). The combined organic layer was dried over MgSO₄, filtered through Celite, and concentrated under reduced pressure. The residue was purified by flash column chromatography (SiO₂, hexane) to give product **S2** (3.95 g, 99%) as a clear oil. ¹H NMR (500 MHz, CDCl₃): δ 7.88 (s, 1H), 7.85 (s, 1H), 7.74 (s, 1H), 7.57 (s, 1H), 5.29 (s, 2H), 5.03 (s, 2H), 4.40 (septet, *J* = 5.0 Hz, 1H), 2.20 (s & m, 8H), 1.91 (m, 2H), 1.16 (m, 22H), 1.03 (m, 2H), 0.84 (t, *J* = 7.0 Hz, 6H). ¹³C NMR (125 MHz, CDCl₃): δ 146.7, 142.2, 138.7, 135.7, 122.8, 121.3, 120.9, 120.7, 119.4, 118.9, 116.3, 115.4, 113.1, 57.1, 33.7, 31.9, 29.5, 29.4, 29.3, 26.9, 24.5, 22.8, 14.3. HR-MALDI: calcd for C₃₅H₅₀Br₂N [*M*+H]⁺ *m/z* = 644.2290; found *m/z* = 644.2261.



1 (3,6-bis(1-methylethenyl)-9-(1-octylonyl)-2,7-bis(4,4,5,5-tetramethyl-1,3,2-dioxaborolan-2-yl)-9*H*-carbazole): Compound **S2** (3.0 g, 4.7 mmol) was dissolved in THF (60 mL) under an nitrogen atmosphere and cooled to $-78\text{ }^{\circ}\text{C}$ in acetone/dry ice bath. To the mixture was added *n*-BuLi (6.1 mL, 9.8 mmol, 1.6M in hexane) slowly. After 30 min stirring at $-78\text{ }^{\circ}\text{C}$, 2-isopropoxy-4,4,5,5-tetramethyl-1,3,2-dioxaborolane (2.3 mL, 11.3 mmol) was added into the mixture. The mixture was warmed to room temperature and stirred at room temperature for 24 h. The reaction mixture was poured into 20 mL of water. THF was removed under reduced pressure, and the residue was extracted with CH_2Cl_2 ($3 \times 30\text{ mL}$). The combined organic layer was dried over MgSO_4 , filtered through Celite, and concentrated under reduced pressure. The residue was purified by flash column chromatography (SiO_2 , hexane/ CH_2Cl_2 100:0 to 50:50) to give product **1** (2.4 g, 70%) as a white solid. ^1H NMR (500 MHz, CDCl_3): δ 7.96 (s, 1H), 7.94 (s, 1H), 7.81 (s, 1H), 7.65 (s, 1H), 5.11 (s, 2H), 4.95 (s, 2H), 4.59 (septet, $J = 5.0\text{ Hz}$, 1H), 2.25 (s & m, 8H), 1.91 (m, 2H), 1.37 (s, 24H), 1.14 (m, 22H) 0.83 (t, $J = 7.0\text{ Hz}$, 1H). ^{13}C NMR (125 MHz, CDCl_3): δ 148.3, 141.3, 139.9, 138.0, 126.1, 125.1, 123.7, 119.2, 119.0, 117.6, 115.0, 113.9, 83.7, 56.5, 34.1, 31.9, 29.7, 29.5, 29.4, 26.9, 25.3, 24.9, 22.8, 14.2. HR-MALDI: calcd for $\text{C}_{47}\text{H}_{74}\text{B}_2\text{NO}_4$ [$M+\text{H}$] $^+$ $m/z = 738.5804$; found $m/z = 738.5804$.



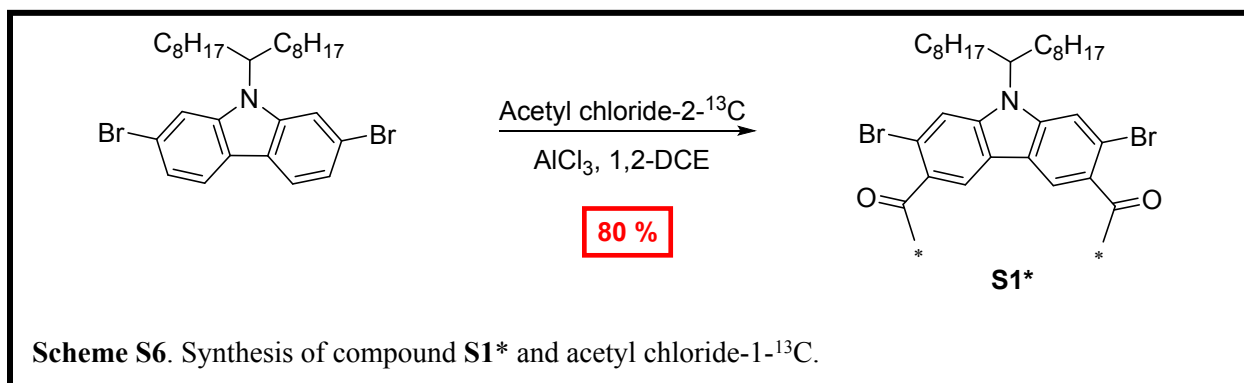
2 (2,7-bis(2-ethenylphenyl)-3,6-bis(1-methylethenyl)-9-(1-octylonyl)-9*H*-carbazole): To a mixture of compound **1** (0.30 g, 0.40 mmol), K₂CO₃ (0.33g, 2.40 mmol), aliquat 336 (0.05 mL, 0.10 mmol), several crystals of 2,6-di-*t*-butyl-4-methylphenol (BHT), and 2-bromostyrene (0.13 mL, 0.96 mmol) in degassed toluene (4 mL) and water (0.8 mL) was added Pd(PPh₃)₄ (46 mg, 10 mol%) under nitrogen atmosphere. The reaction mixture was stirred at 100 °C for 24 h. After being cooled to room temperature, the reaction mixture was concentrated under reduced pressure, and the residue was extracted with DCM (3 × 10 mL). The combined organic layer was dried over MgSO₄, filtered through Celite, and concentrated under reduced pressure. The residue was purified by flash column chromatography (SiO₂, hexane). The product was further purified by preparative GPC to give product **2** (0.21 g, 77 %) as a light yellow sticky oil. ¹H NMR (500 MHz, CDCl₃): δ 8.08 (s, 1H), 8.05(s, 1H), 7.68 (d, *J* = 7.5 Hz, 2H), 7.37 (m, 4H), 7.30 (m, 3H), 7.15 (s, 1H), 6.59 (m, 2H), 5.66 (d, *J* = 17.5 Hz, 2H), 5.08 (s, 2H), 5.02 (s, 2H), 4.93 (s, 2H), 4.44 (septet, *J* = 5.0 Hz, 1H), 2.18 (m, 2H), 1.79 (m, 2H), 1.75 (s, 6H), 1.18 (m, 22H), 1.03 (m, 2H), 0.82 (t, *J* = 7.0 Hz, 1H). ¹³C NMR (125 MHz, CDCl₃): δ 146.7, 142.1, 141.9, 141.5, 138.0, 136.4, 136.3, 136.1, 136.0, 135.8, 134.8, 131.0, 127.3, 127.1, 125.2, 125.0, 122.9, 121.5, 120.2, 119.9, 115.7, 114.2, 111.6, 55.7, 33.8, 31.9, 29.6, 29.5, 29.3, 27.1, 26.9, 24.1, 22.8, 14.2. HR-MALDI: calcd for C₅₁H₆₄N [M+H]⁺ *m/z* = 690.5039; found *m/z* = 690.5065.



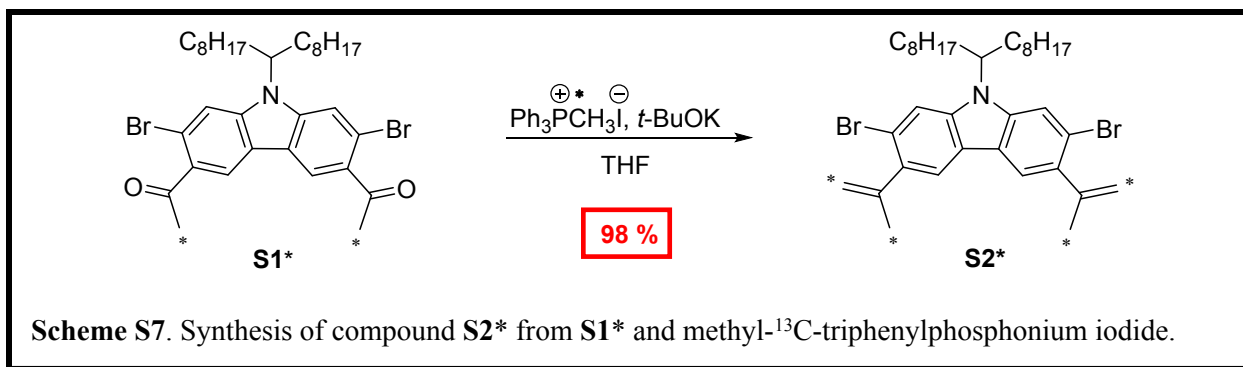
3 (6,9-dimethyl-16-(1-octylonyl)-16*H*-dinaphtho[1,2-*b*:2',1'-*h*]-carbazole): The mixture of compound **2** (100 mg, 0.14 mmol) and Grubbs' 2nd generation catalyst (3 mg, 3 mol%) in degassed toluene (5 mL) was stirred at reflux under N₂. Immediately, another portion of Grubbs' 2nd generation catalyst (9 mg, 7 mol%) in degassed toluene (3 mL) was added for 4 h using syringe pump. After that, the reaction mixture was stirred for an additional 2 h at reflux temperature. After being cooled to room temperature, the reaction mixture was concentrated under reduced pressure, and the residue was purified by flash column chromatography (SiO₂, hexane:CH₂Cl₂ 98:2 to 84:16) to give product **3** (85 mg, 96 %) as a yellow solid. ¹H NMR (500 MHz, CDCl₃): δ 8.97 (s, 1H), 8.94 (s, 1H), 8.86 (s, 1H), 8.82 (d, *J* = 8.0 Hz, 1H), 8.77 (d, *J* = 8.0 Hz, 1H), 8.67 (s, 1H), 7.86 (d, *J* = 7.5 Hz, 2H), 7.65 (m, 2H), 7.60 (t, *J* = 7.5 Hz, 2H), 7.54 (s, 2H), 4.98 (septet, *J* = 5.0 Hz, 1H), 2.98 (s, 6H), 2.65 (m, 2H), 2.16 (m, 2H), 1.33 (m, 4H), 1.26 (m, 2H), 1.07 (m, 18H), 0.72

(t, $J = 7.0$ Hz, 6H). ^{13}C NMR (125 MHz, CDCl_3): δ 143.7, 140.1, 133.2, 132.5, 130.4, 129.9, 128.1, 126.6, 126.0, 125.5, 124.9, 124.2, 124.1, 123.8, 122.7, 116.4, 116.3, 103.4, 100.7, 56.8, 33.8, 30.2, 29.9, 29.7, 29.5, 29.3, 27.1, 22.7, 20.8, 14.1. HR-MALDI: calcd for $\text{C}_{47}\text{H}_{56}\text{N}$ $[M+\text{H}]^+$ $m/z = 634.4413$; found $m/z = 634.4427$. Single crystal X-ray diffraction data are described in section 15.

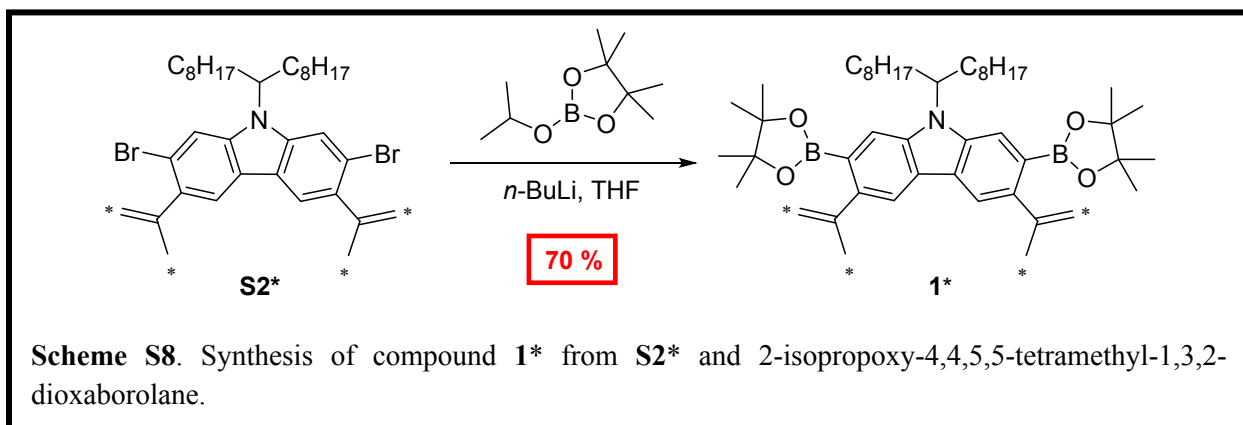
3. Synthesis of ^{13}C Labeled Compounds



S1*: The same reaction and purification procedure for the synthesis of **S1** was followed using acetyl chloride-2- ^{13}C as a carbon-13 source (99% ^{13}C isotope enriched). Yield: 1.3 g (80 %). ^1H NMR (500 MHz, CDCl_3): δ 8.34 (s, 1H), 8.34 (s, 1H), 7.82 (s, 1H), 7.65 (s, 1H), 4.45 (septet, $J = 5.0$ Hz, 1H), 2.77 (d, $^1J_{\text{C-H}} = 128.5$ Hz, 6H), 2.19 (m, 2H), 1.93 (m, 2H), 1.18 (m, 22H), 0.95 (m, 2H), 0.82 (t, $J = 7.0$ Hz, 6H). ^{13}C NMR (125 MHz, CDCl_3): δ 200.1, 144.5, 141.1, 132.6, 132.5, 122.5, 121.0, 118.2, 117.5, 117.3, 115.1, 57.8, 33.6, 31.8, 30.5 (^{13}C enriched), 29.4, 29.2, 26.8, 22.7, 14.2. HR-MALDI: calcd for $\text{C}_{33}\text{H}_{45}\text{Br}_2\text{NO}_2$ $[M+\text{H}]^+$ $m/z = 650.1943$; found $m/z = 650.1907$.

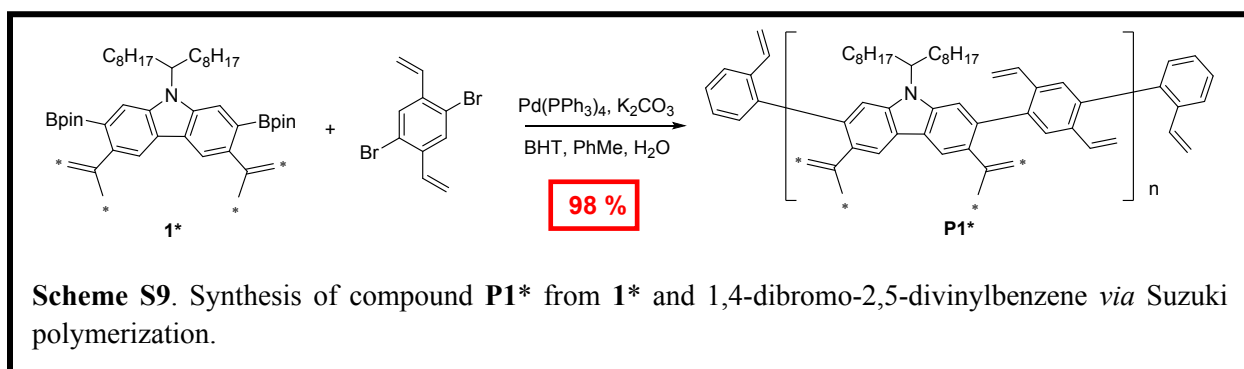


S2*: The same reaction and purification procedure for the synthesis of **S2** was followed using methyl-¹³C-triphenylphosphonium iodide as a carbon-13 source (99% ¹³C isotope enriched). Yield: 0.60 g (98 %). ¹H NMR (500 MHz, CDCl₃): δ 7.88 (s, 1H), 7.85 (s, 1H), 7.74 (s, 1H), 7.57 (s, 1H), 5.29 (dd, ¹J_{C-H} = 156.0 Hz, ³J_{C-H} = 6.0 Hz, 2H), 5.03 (dd, ¹J_{C-H} = 157.0 Hz, ³J_{C-H} = 11.0 Hz, 2H), 4.40 (septet, *J* = 5.0 Hz, 1H), 2.20 (dd, ¹J_{C-H} = 127.0 Hz, ³J_{C-H} = 5.5 Hz, 6H), 2.20 (m, 2H), 1.91 (m, 2H), 1.16 (m, 22H), 1.03 (m, 2H), 0.84 (t, *J* = 7.0 Hz, 6H). ¹³C NMR (125 MHz, CDCl₃): δ 146.7, 142.2, 138.7, 135.7, 122.8, 121.3, 120.9, 120.7, 119.4, 118.9, 116.3 (¹³C enriched), 115.4, 113.1, 57.1, 33.7, 31.9, 29.5, 29.4, 29.3, 26.9, 24.5 (¹³C enriched), 22.8, 14.3. HR-MALDI: calcd for C₃₃H₄₅Br₂NO₂ [*M*+H]⁺ *m/z* = 648.2425; found *m/z* = 648.1810.

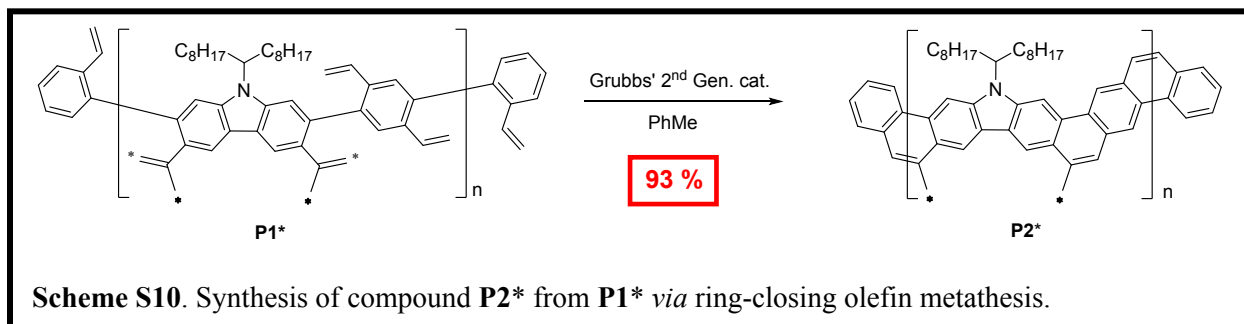


1*: The same reaction and purification procedure for the synthesis of **1** was followed. Yield: 0.28 g (70 %). ¹H NMR (500 MHz, CDCl₃): δ 7.96 (s, 1H), 7.94 (s, 1H), 7.81 (s, 1H), 7.65 (s, 1H),

5.11 (dd, $^1J_{C-H} = 155.0$ Hz, $^3J_{C-H} = 6.0$ Hz, 2H), 4.95 (dd, $^1J_{C-H} = 155.0$ Hz, $^3J_{C-H} = 11.0$ Hz, 2H), 4.59 (septet, $J = 5.0$ Hz, 1H), 2.25 (dd, $^1J_{C-H} = 126.5$ Hz, $^3J_{C-H} = 5.5$ Hz, 6H), 2.25 (m, 2H), 1.91 (m, 2H), 1.37 (s, 24H), 1.14 (m, 22H) 0.83 (t, $J = 7.0$ Hz, 1H). ^{13}C NMR (125 MHz, $CDCl_3$): δ 148.3, 141.3, 139.9, 138.0, 126.1, 125.1, 123.7, 119.2, 119.0, 117.6, 115.0, 113.9 (^{13}C enriched), 83.7, 56.5, 34.1, 31.9, 29.7, 29.5, 29.4, 26.9, 25.3 (^{13}C enriched), 24.9, 22.8, 14.2. HR-MALDI: calcd for $C_{47}H_{73}B_2NO_4 [M+H]^+$ $m/z = 742.5940$; found $m/z = 742.5876$.



P1*: The same reaction and purification procedure for the synthesis of **P1** was followed. Yield: 98 %. ($M_n = 6$ kg/mol, PDI = 2.4). **P1*** was further subjected to preparative recycling SEC to remove oligomers (0.45 g, 74 %, $M_n = 17$ kg/mol, PDI = 1.37 by SEC).



P2*: The same reaction and purification procedure for the synthesis of **P2** was followed. Yield: 93% (M_n : 13 kg/mol, PDI: 1.71 by SEC).

4. Ring-closing Olefin Metathesis Optimization.

Screened conditions for ring-closing olefin metathesis are summarized in **Table S1**. In preliminary screening for the synthesis of **3**, higher temperature afforded better yield (**Entry 1–4**). The condition at high temperature for **3**, however, was not enough to convert vinyl groups into aromatic rings quantitatively (**Entry 3-4**), probably due to the thermal decomposition of Grubbs' 2nd generation catalyst.⁶ Therefore, several different ways for the addition of the catalyst were tried (**Entry 5–11**). The optimized condition requires the addition of the catalyst in toluene solution over 4 hr at reflux temperature slowly using syringe pump, followed by stirring the reaction mixture at reflux temperature for an additional 2 hours (**Entry 5**). Using the optimized condition, **P1** was converted to **P2** in 91% yield.

Table S1. The optimization of ring-closing olefin metathesis.

Entry	Product	Catalyst (mol %) ^a	Addition of catalyst	Solvent	Temp. (°C)	Time (h)	Yield (%)
1	3	10 ^b	1 portion	CH ₂ Cl ₂	35	24	39 ^c
2	3	10	1 portion	CH ₂ Cl ₂	35	24	54 ^c
3	3	10	1 portion	PhMe	100	24	69 ^c
4	3	10	1 portion	PhMe	reflux	24	77 ^c
5	3	10	Syringe pump for 4 h	PhMe	reflux	6	96 ^c
6	P2	10	1 portion	PhMe	reflux	24	44 ^d
7	P2	20	1 portion	PhMe	reflux	24	71 ^d
8	P2	20	2 portions in 12 h	PhMe	reflux	24	89 ^d

9	P2	20	4 portions in 6 h	PhMe	reflux	24	quant. ^{d, e}
10	P2	20	Syringe pump for 4 h	PhMe	reflux	6	91 ^c quant. ^{d, e}
11	P2	20	Syringe pump For 6 h	PhMe	reflux	8	quant. ^{d, e}

^a Grubbs' 2nd generation catalyst was used. ^b Grubbs' 1st generation catalyst was used ^c Isolated yield. ^d Conversion yield calculated by ¹H NMR based on the integration ratio between vinyl peaks on 6.75 (2H) and 5.69 ppm (2H) and newly appeared aromatic peaks on 9.03 ppm (5H). ^e Too small amount of unreacted defect which was difficult to integrate was observed.

5. Size Exclusion Chromatography (SEC)

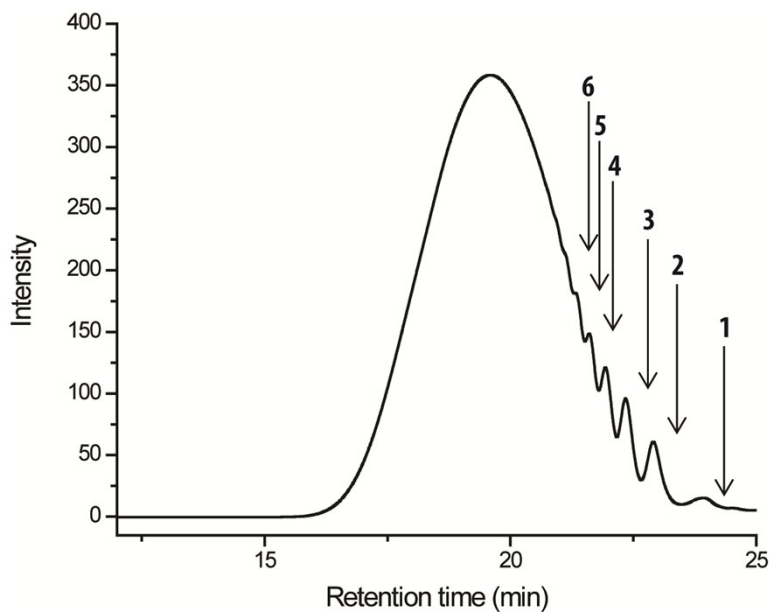


Figure S1. Size exclusion chromatogram of **P1** before purified by preparative recycling SEC. The oligomers generated in this step-growth polymerization can be clearly identified (the numbered arrows).

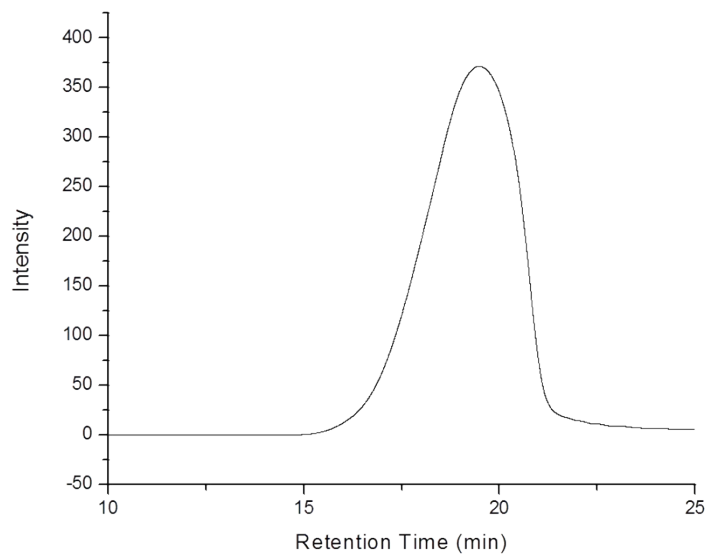


Figure S2. Size exclusion chromatogram of **P1** after purified by preparative recycling SEC.

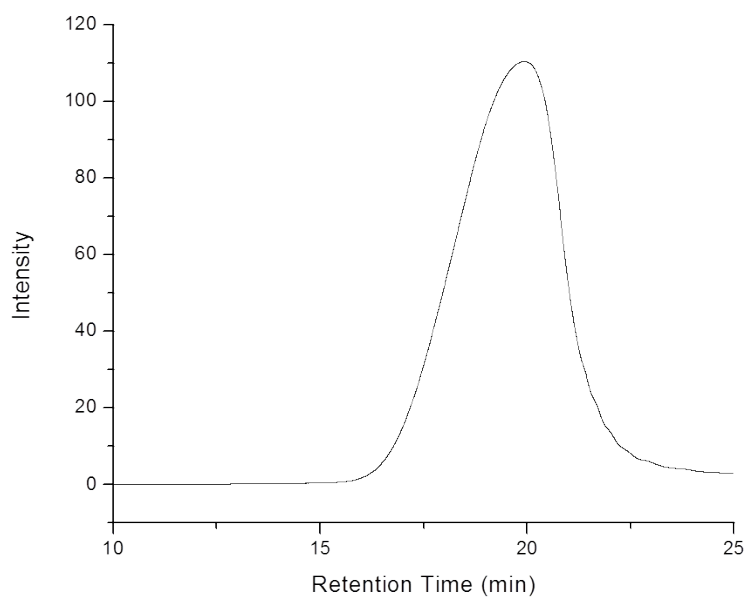


Figure S3. Size exclusion chromatogram of **P2**.

6. IR Spectra

FT-IR spectra of **2**, **3**, **P1**, and **P2** were recorded neat on an ZnSe Attenuated Total Reflection (ATR) apparatus. Alkenyl stretching peaks are indicated as a red arrow. The disappearance of C=C stretching peak (3080 cm^{-1}) and =C-H stretching peak (1626 cm^{-1}) of **2** is indicated as a dashed circle (red) in the spectrum of **3**. The same trend was also observed between **P1** and **P2**. The disappearance of C=C stretching peak (3080 cm^{-1}) and =C-H stretching peak (1624 cm^{-1}) of **P1** is indicated as a dashed circle (red) in the spectrum of **P2**.

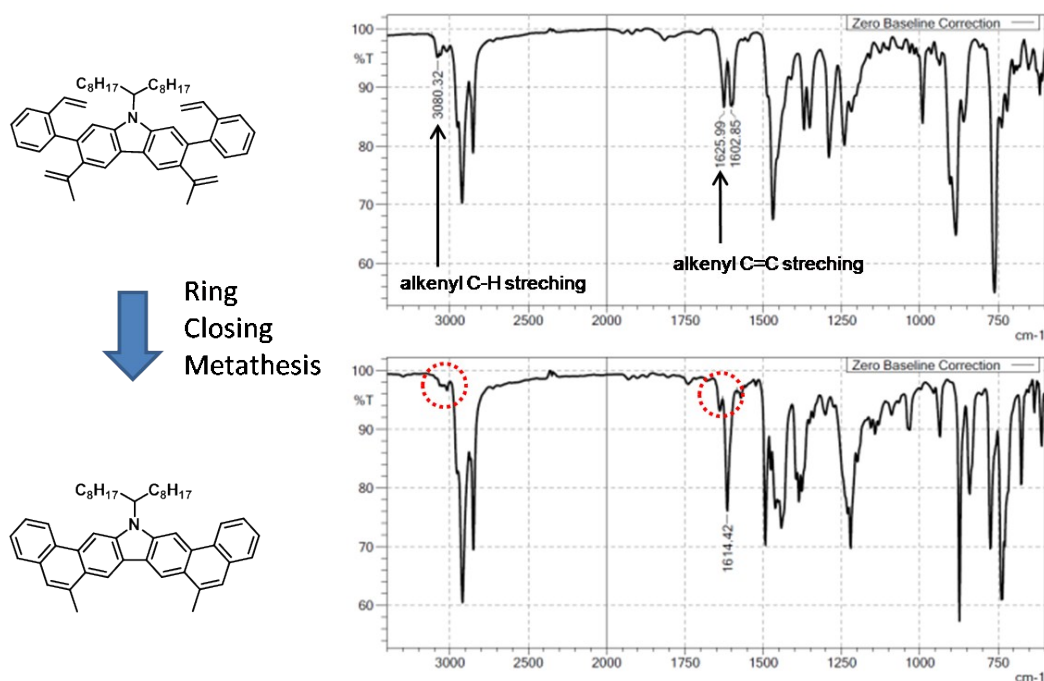


Figure S4. IR spectra comparison of **2** and **3**.

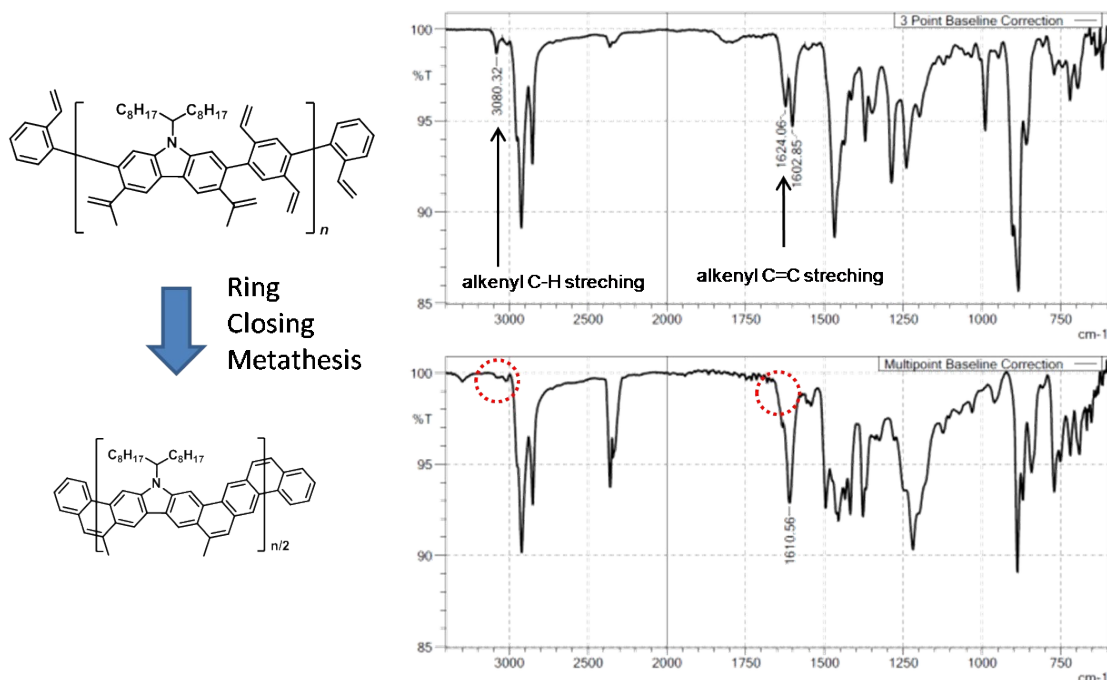


Figure S5. IR spectra comparison of **P1** and **P2**.

7. ¹H-¹H NOESY Spectrum of **3**

In order to fully assign the proton peaks of **3**, ¹H-¹H NOESY was recorded at room temperature in CDCl₃. The sample solution was degassed by freeze-pump-thaw 3 times before the experiment. The experiment was performed after 90° pulse width calibration. Each proton peaks were assigned based on the observed correlation signals (marked as double head arrows).

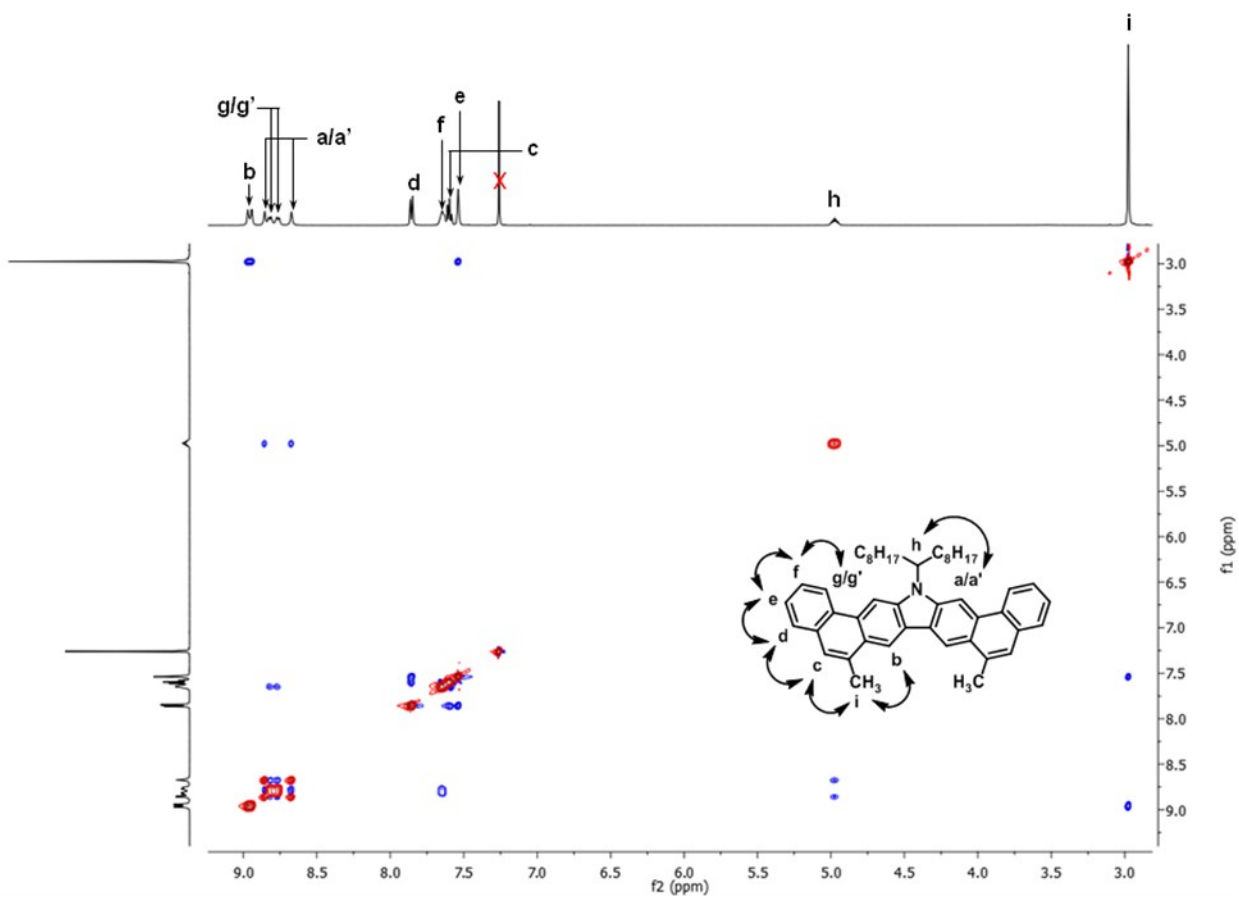


Figure S6. Partial ^1H - ^1H NOESY spectrum of **3** (500 MHz, CDCl_3 , RT). Double head arrows in the figure indicate the observed through space nuclear overhauser effect in the experiment.

8. ^1H and ^{13}C NMR Spectra

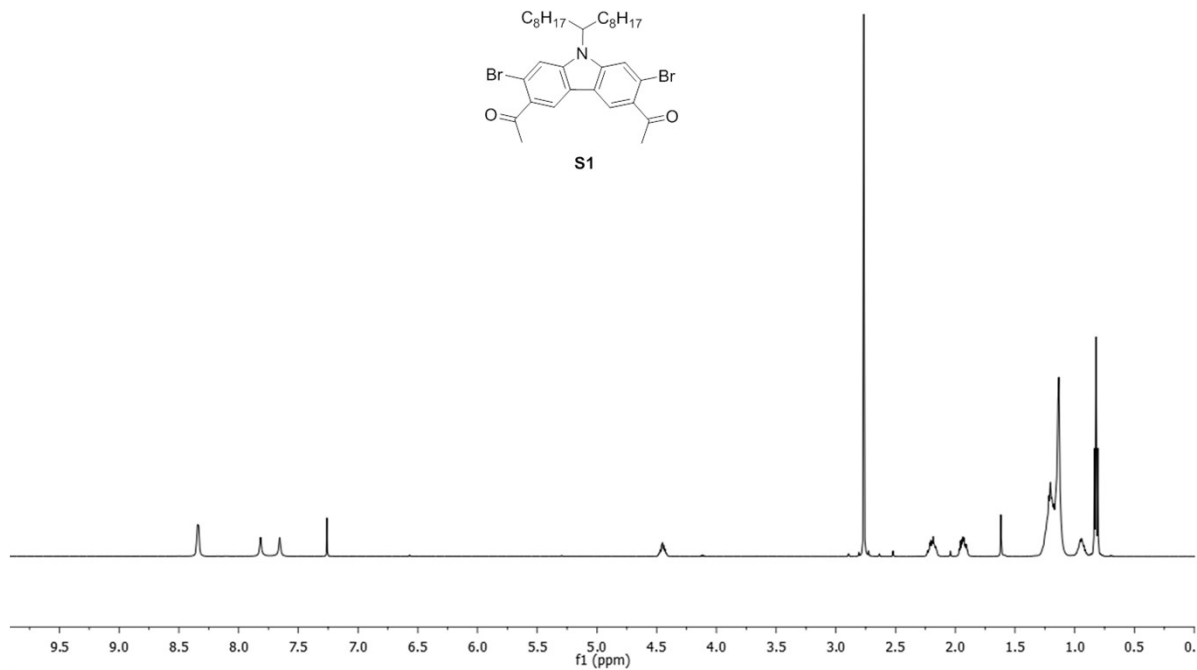


Figure S7. ^1H NMR of S1 (500 MHz, CDCl_3 , RT).

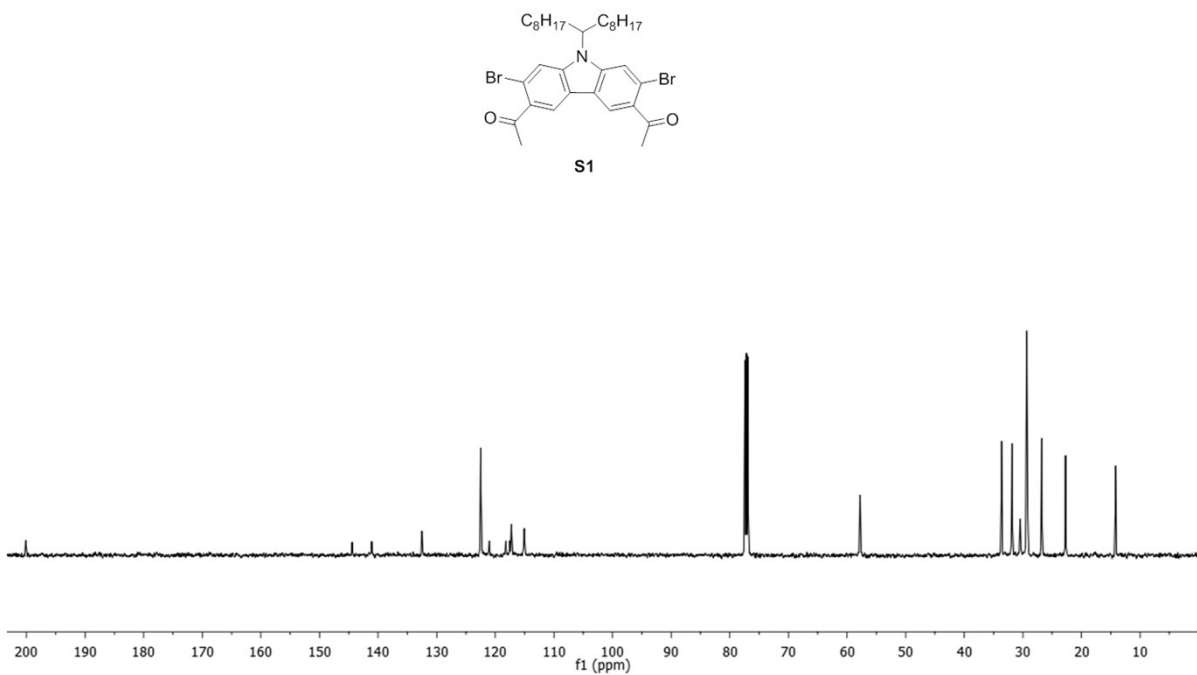


Figure S8. ^{13}C NMR of S1 (125 MHz, CDCl_3 , RT).

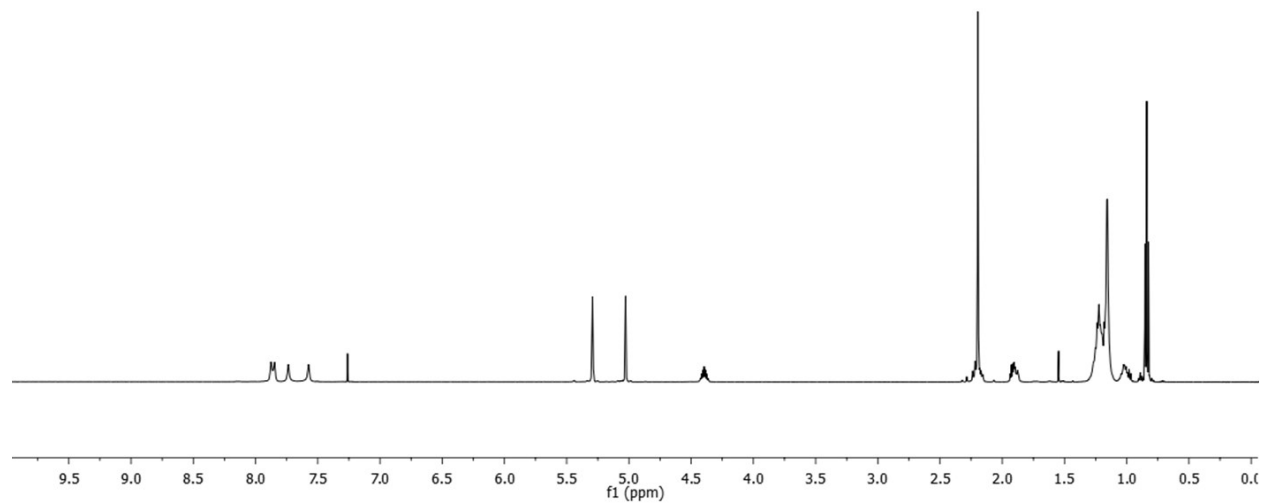
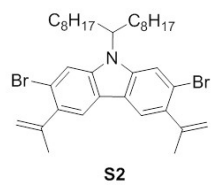


Figure S9. ¹H NMR of S2 (500 MHz, CDCl₃, RT).

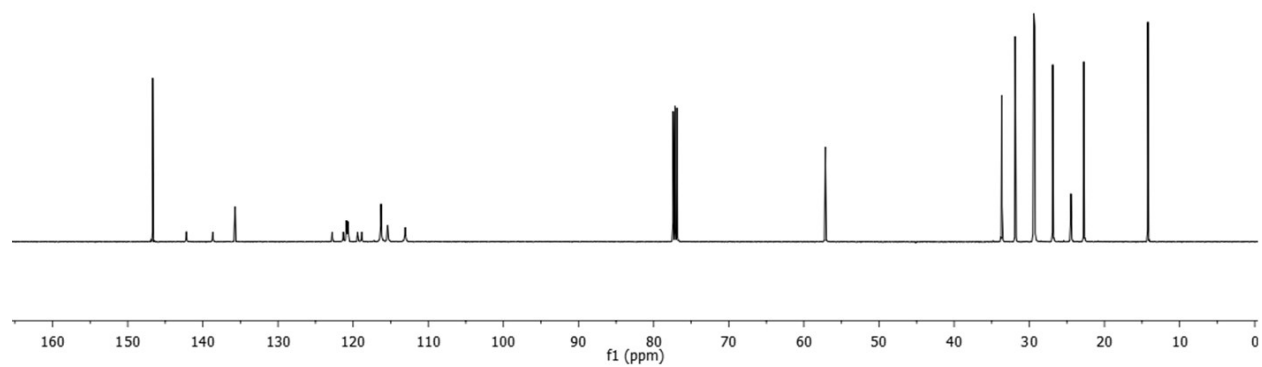
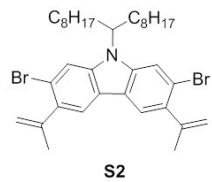


Figure S10. ¹³C NMR of S2 (125 MHz, CDCl₃, RT).

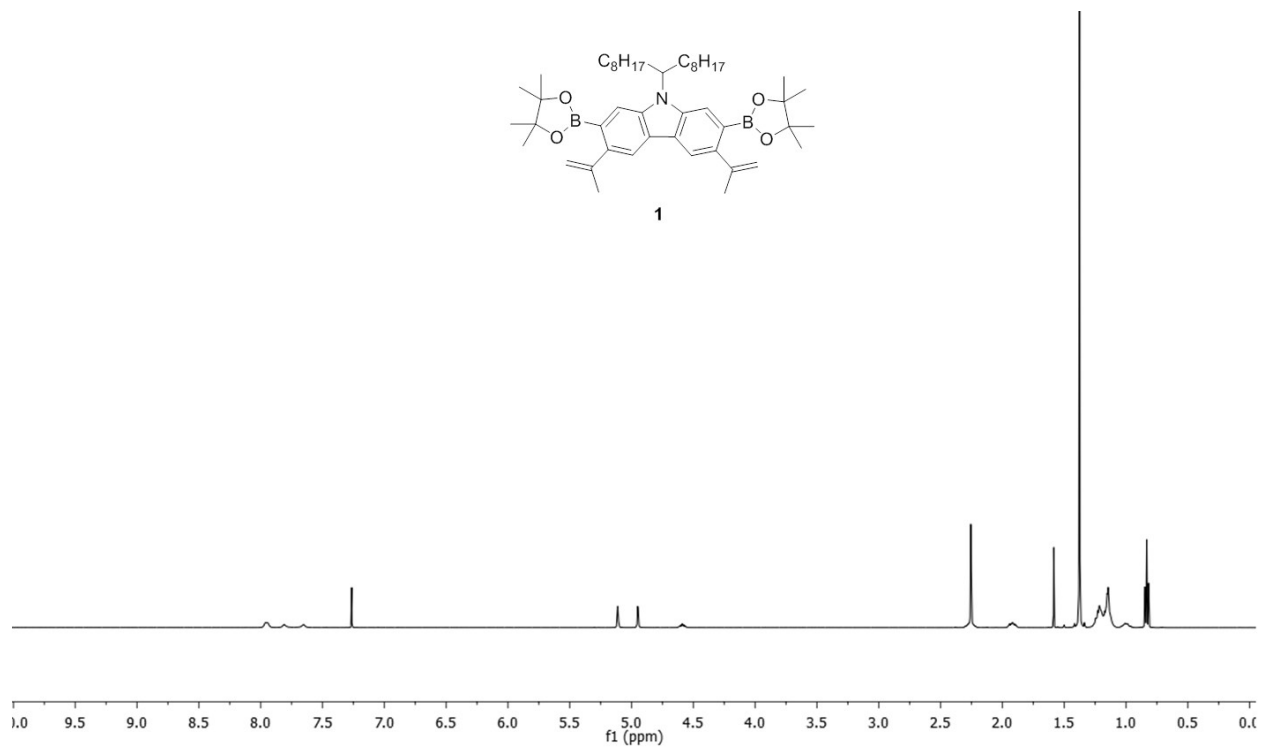


Figure S11. 1H NMR of **1** (500 MHz, $CDCl_3$, RT).

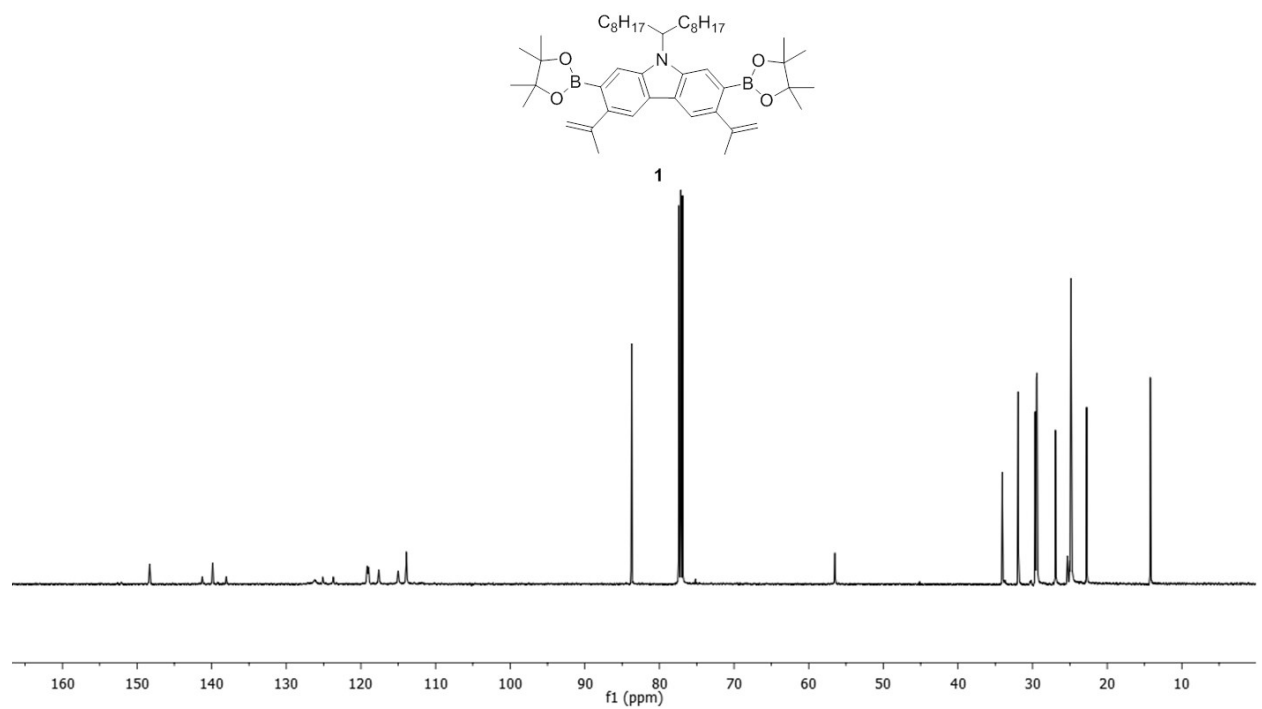


Figure S12. ^{13}C NMR of **1** (125 MHz, $CDCl_3$, RT).

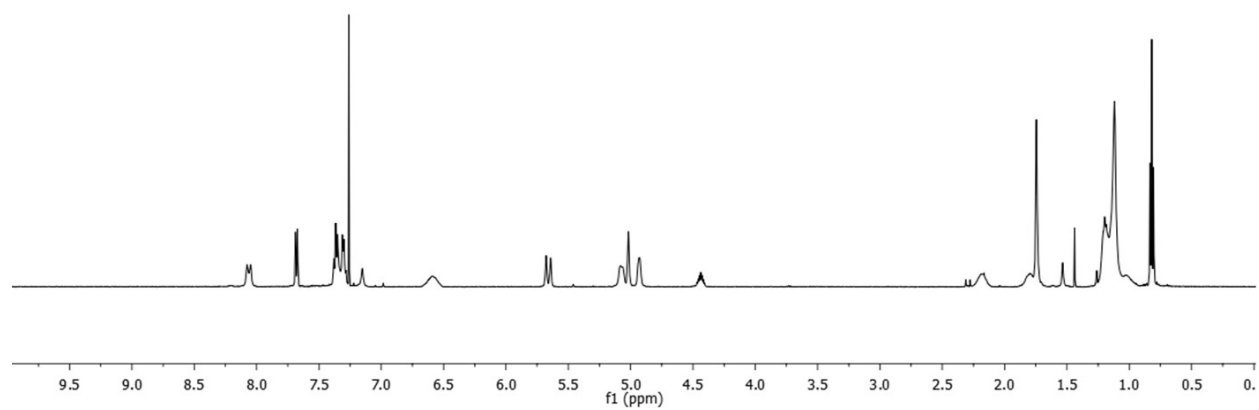
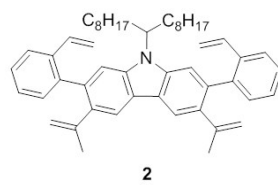


Figure S13. 1H NMR of **2** (500 MHz, $CDCl_3$, RT).

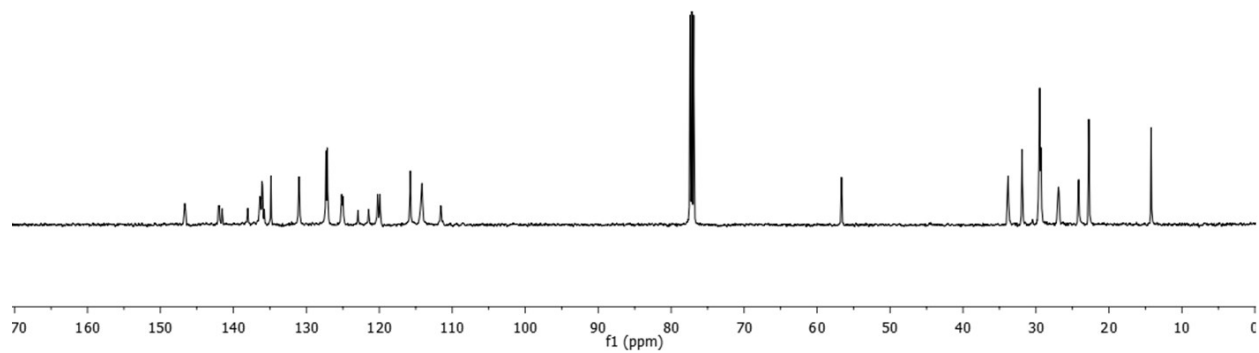
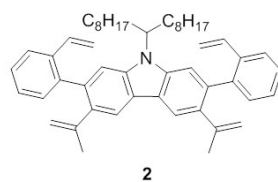


Figure S14. ^{13}C NMR of **2** (125 MHz, $CDCl_3$, RT).

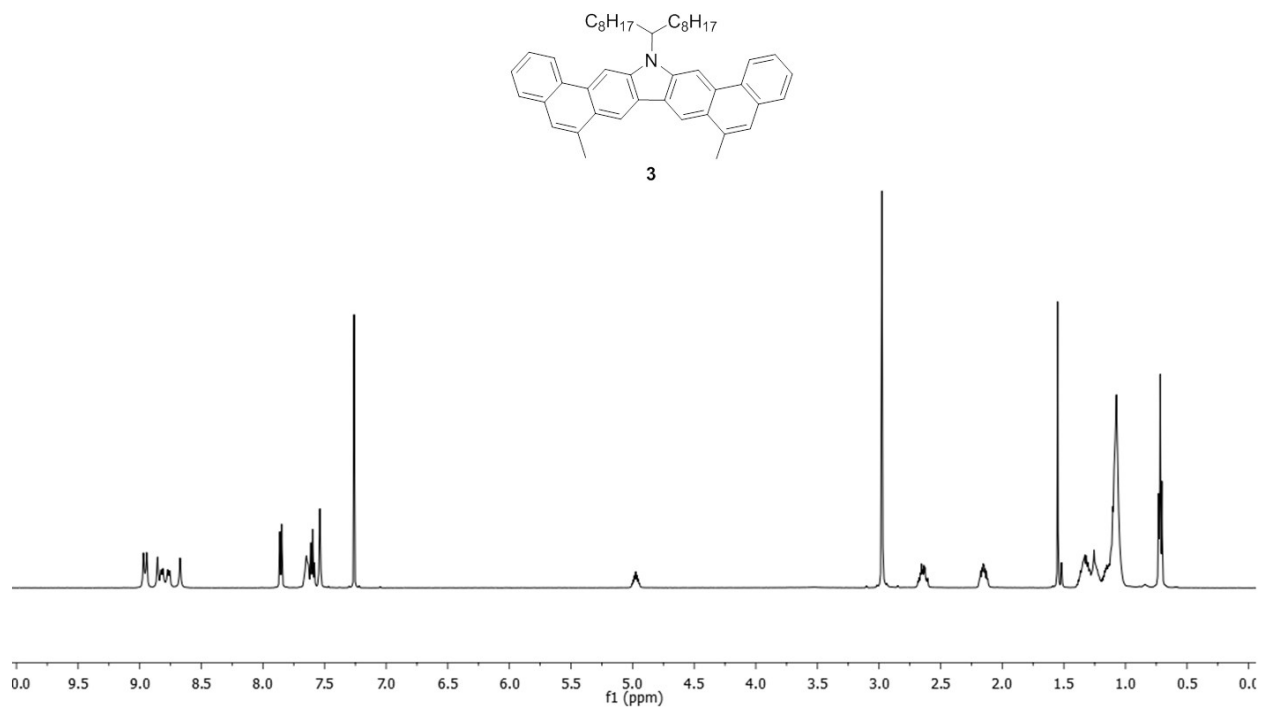


Figure S15. ^1H NMR of **3** (500 MHz, CDCl_3 , RT).

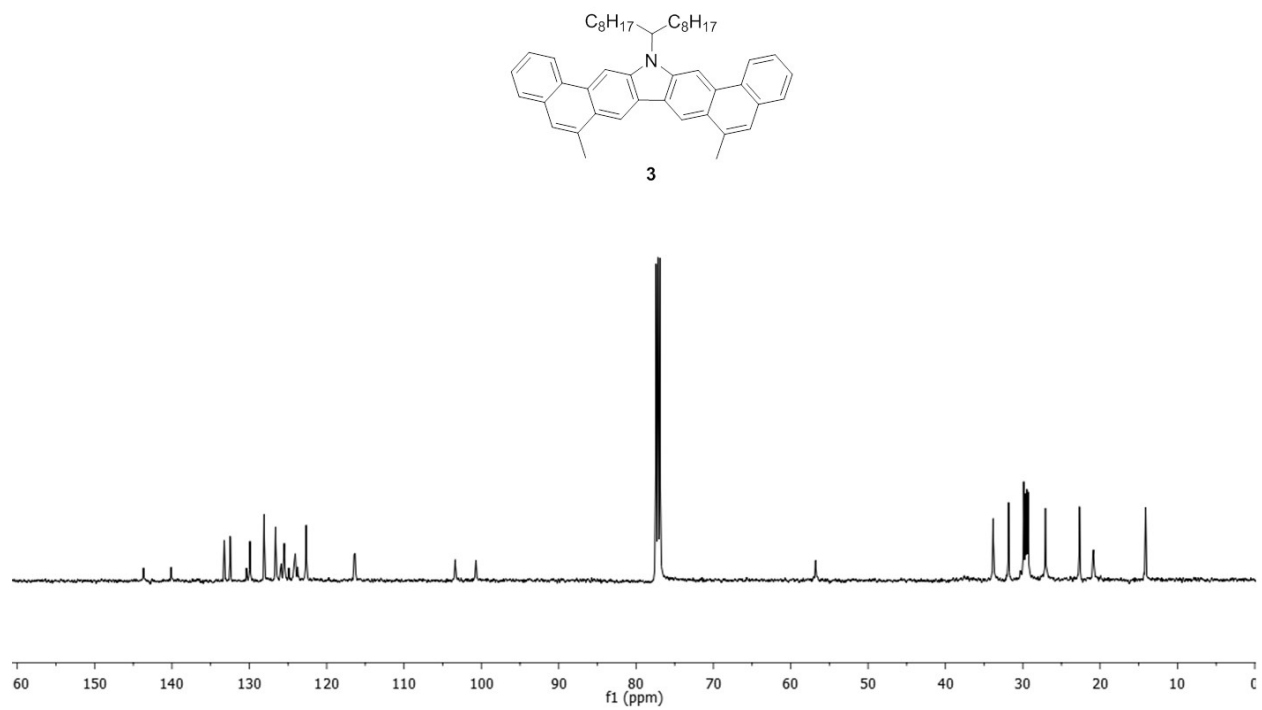


Figure S16. ^{13}C NMR of **3** (125 MHz, CDCl_3 , RT).

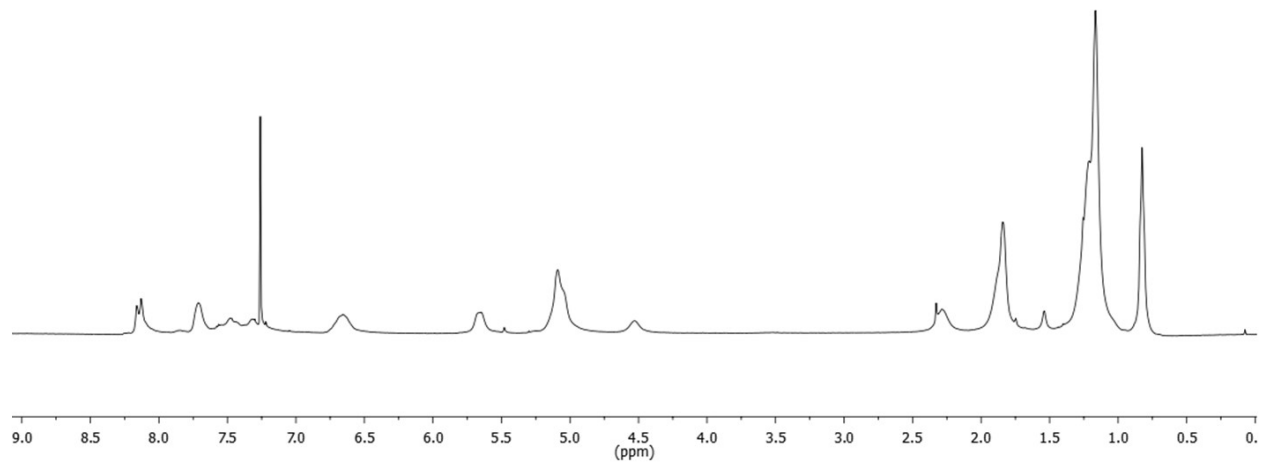
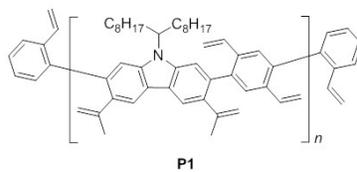


Figure S17. ^1H NMR of **P1** (500 MHz, CDCl_3 , RT).

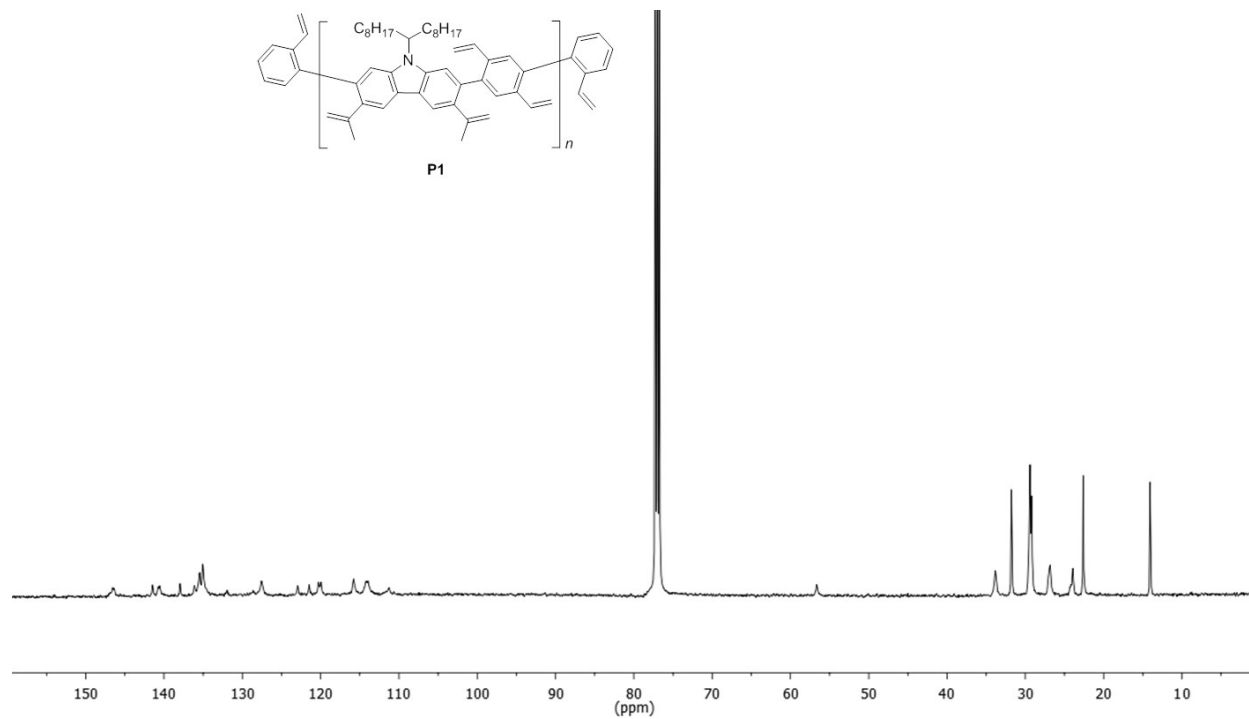


Figure S18. ^{13}C NMR of **P1** (125 MHz, CDCl_3 , RT).

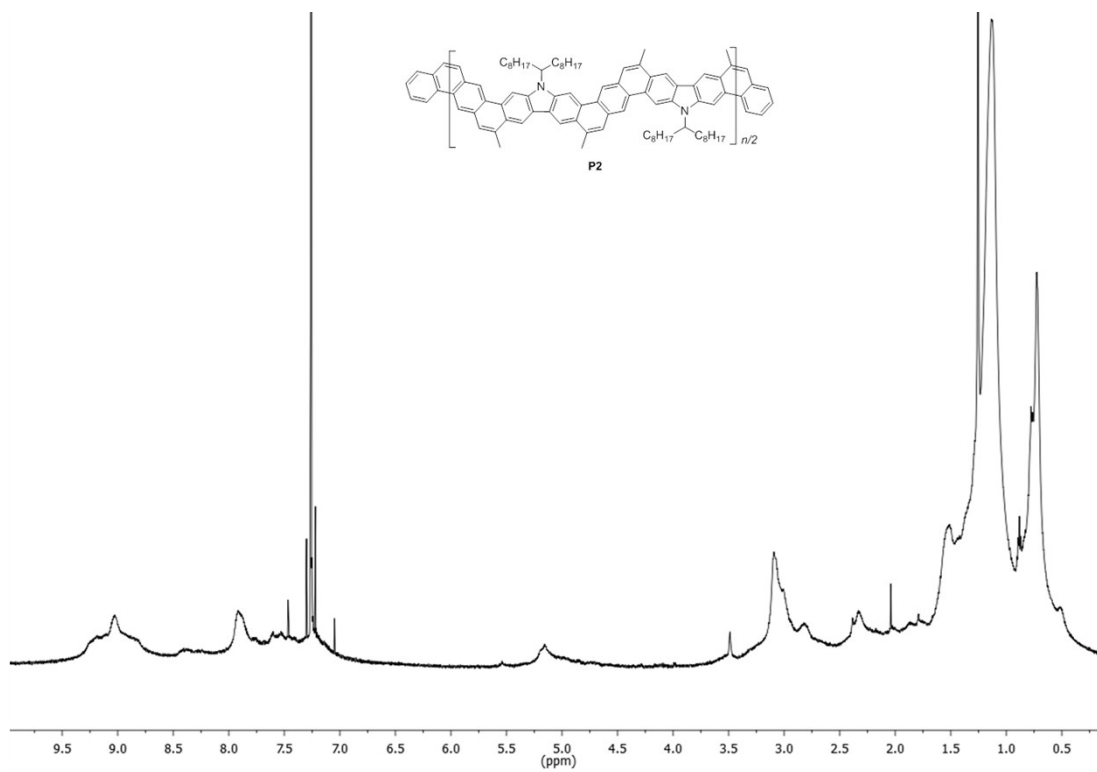


Figure S19. ^1H NMR of **P2** (500 MHz, CDCl_3 , RT).

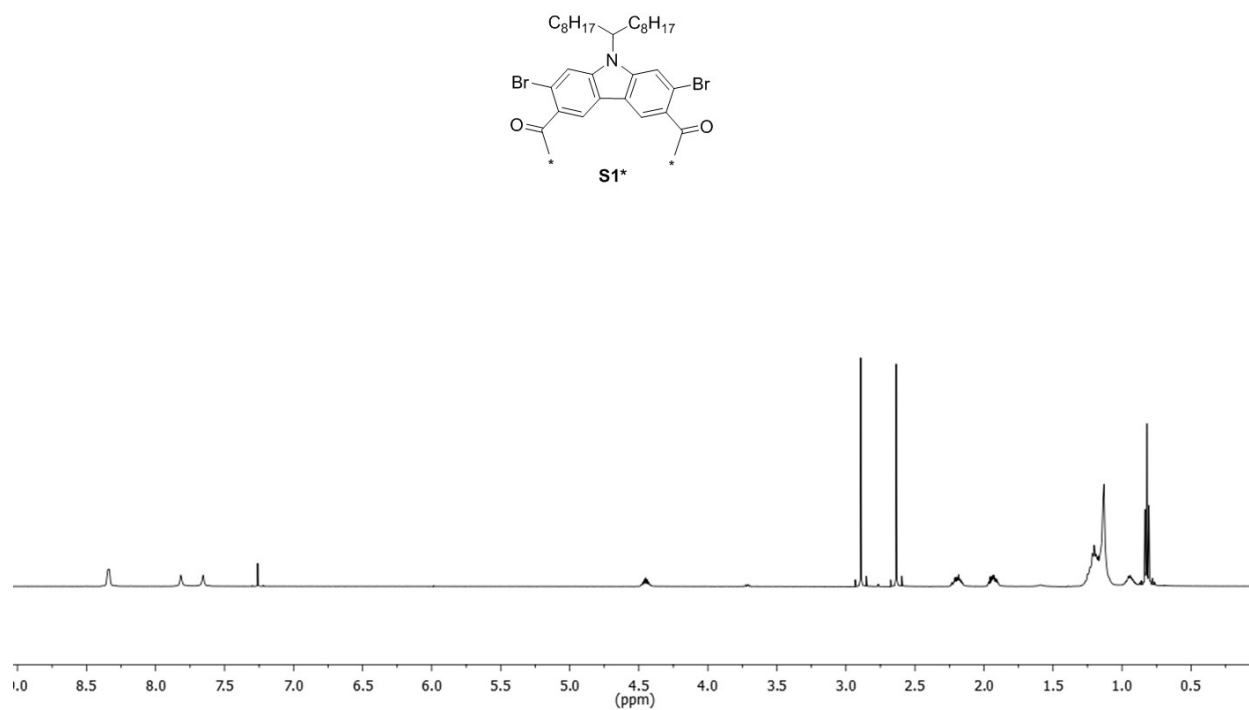


Figure S20. ^1H NMR of **S1*** (500 MHz, CDCl_3 , RT).

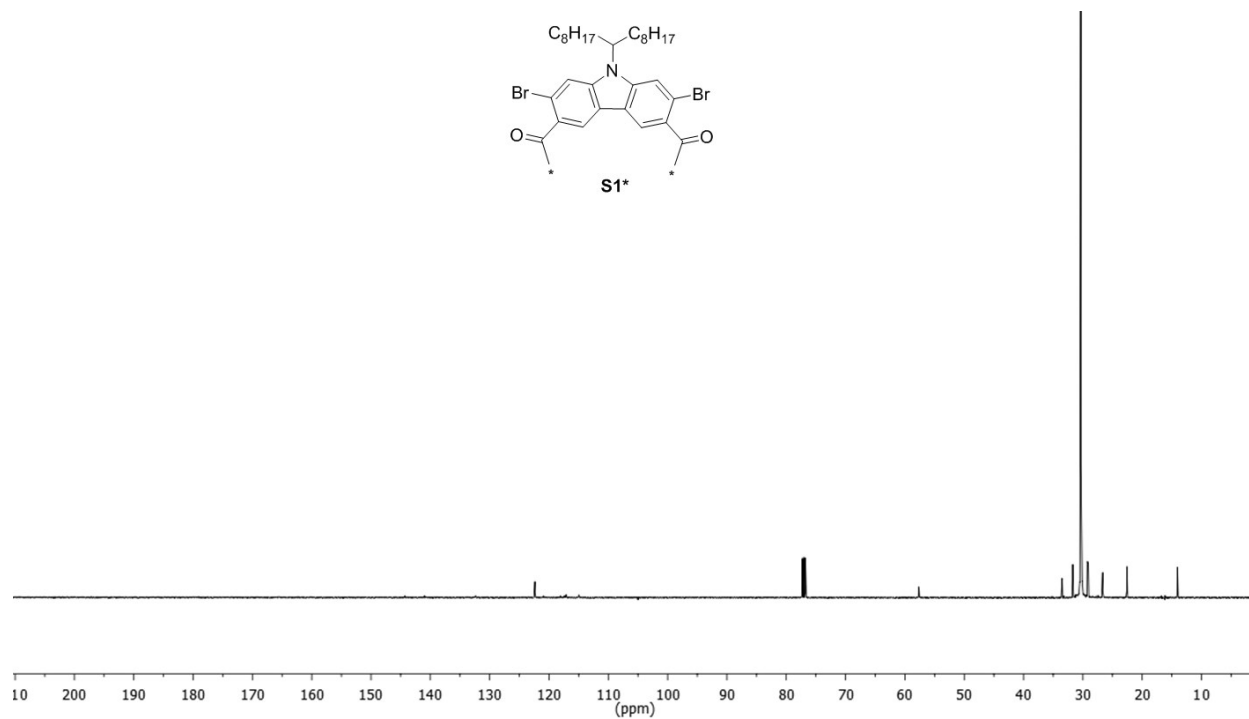


Figure S21. ¹³C NMR of S1* (125 MHz, CDCl₃, RT).

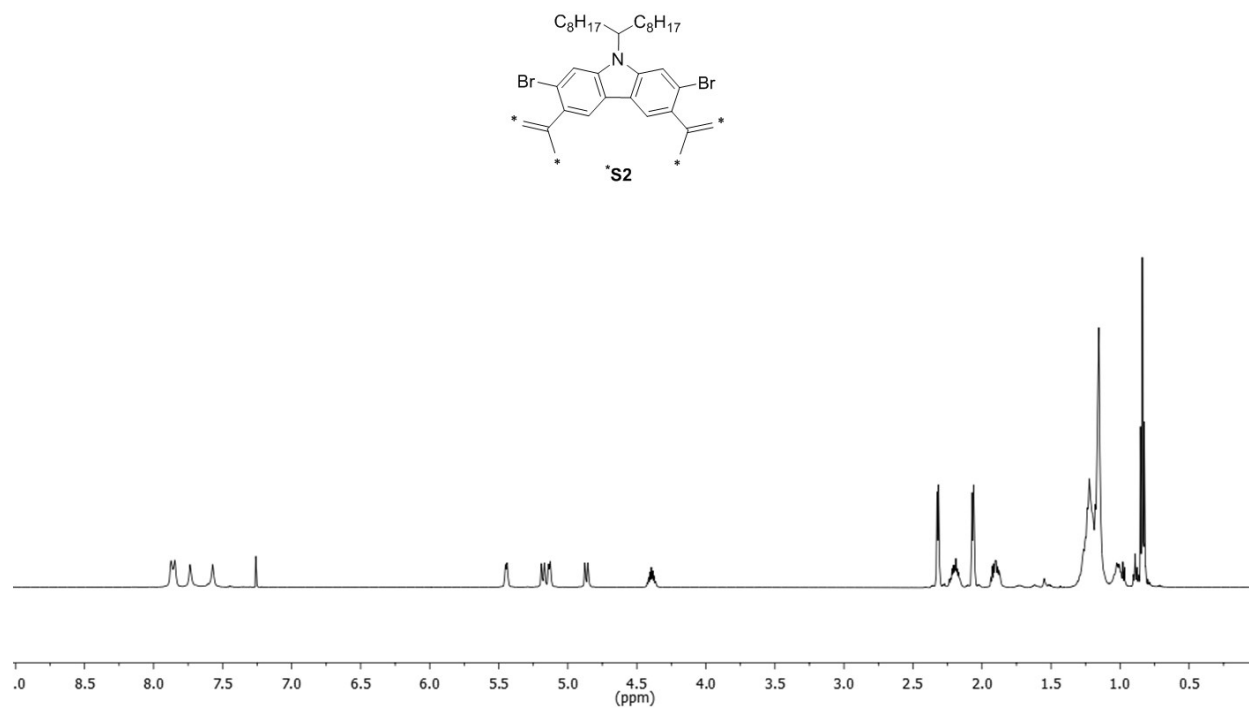


Figure S22. ¹H NMR of S2* (500 MHz, CDCl₃, RT).

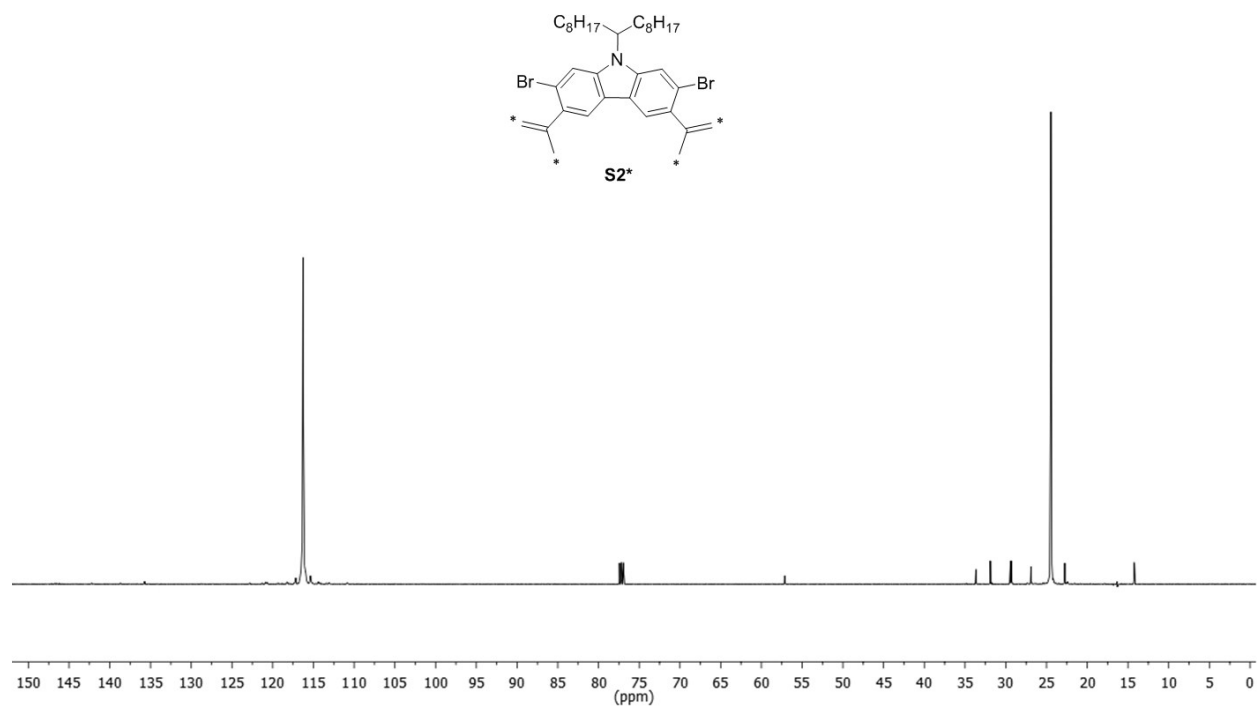


Figure S23. ¹³C NMR of **S2*** (125 MHz, CDCl₃, RT).

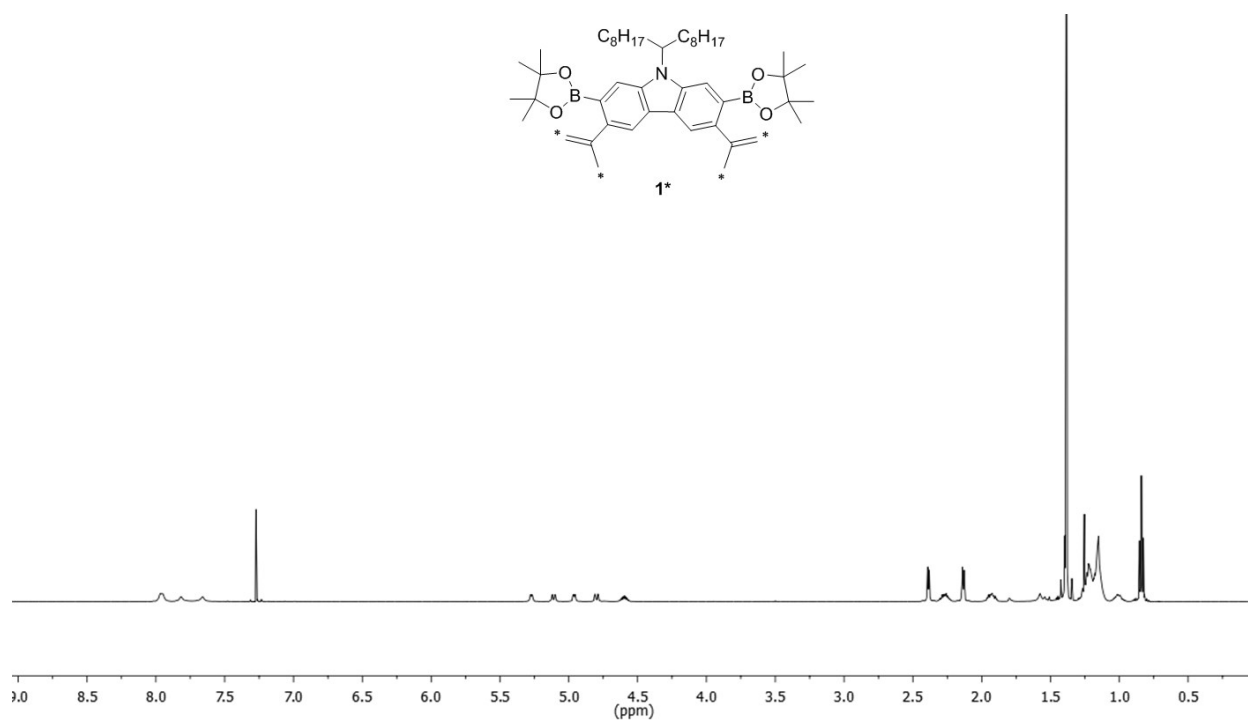


Figure S24. ¹H NMR of **1*** (500 MHz, CDCl₃, RT).

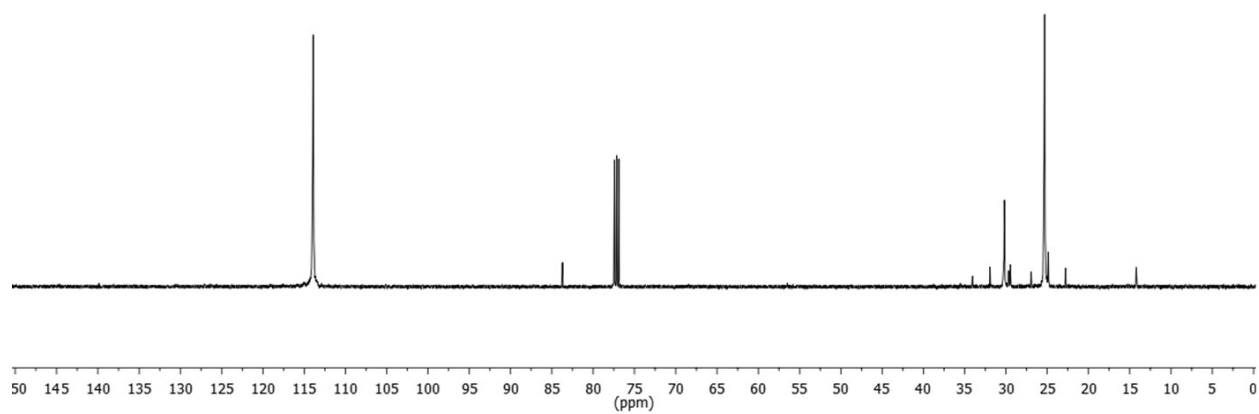
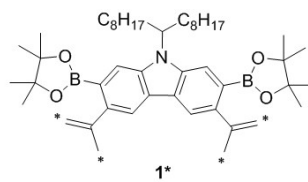


Figure S25. ^{13}C NMR of **1*** (125 MHz, $CDCl_3$, RT).

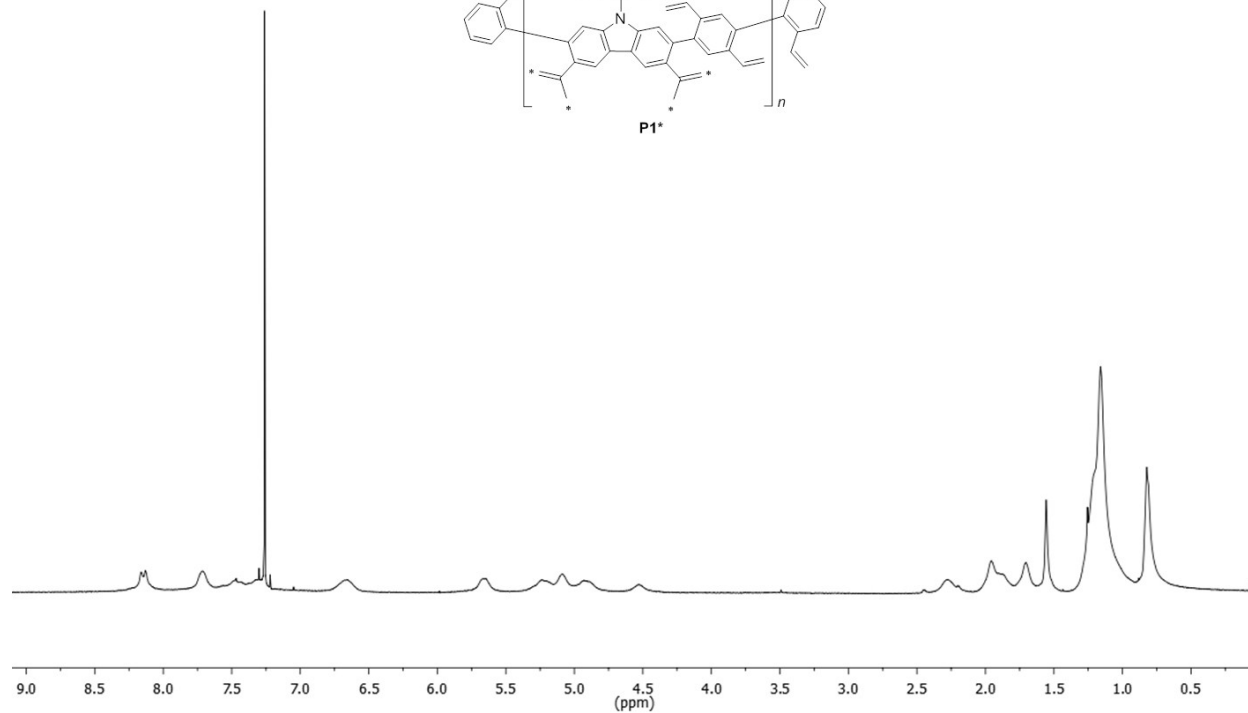
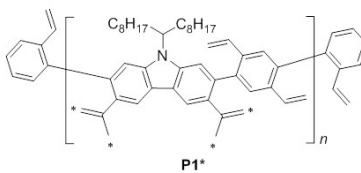


Figure S26. 1H NMR of **P1*** (500 MHz, $CDCl_3$, RT).

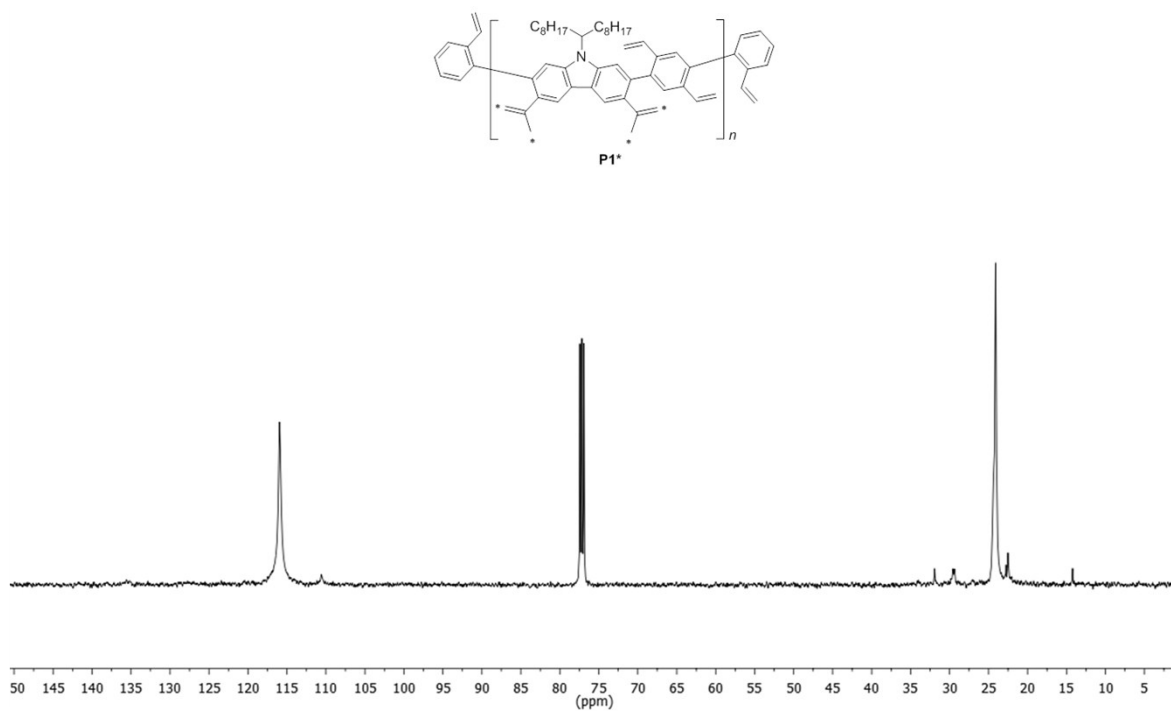


Figure S27. ^{13}C NMR of **P1*** (125 MHz, CDCl_3 , RT). S/N ratio of the spectrum is 94.

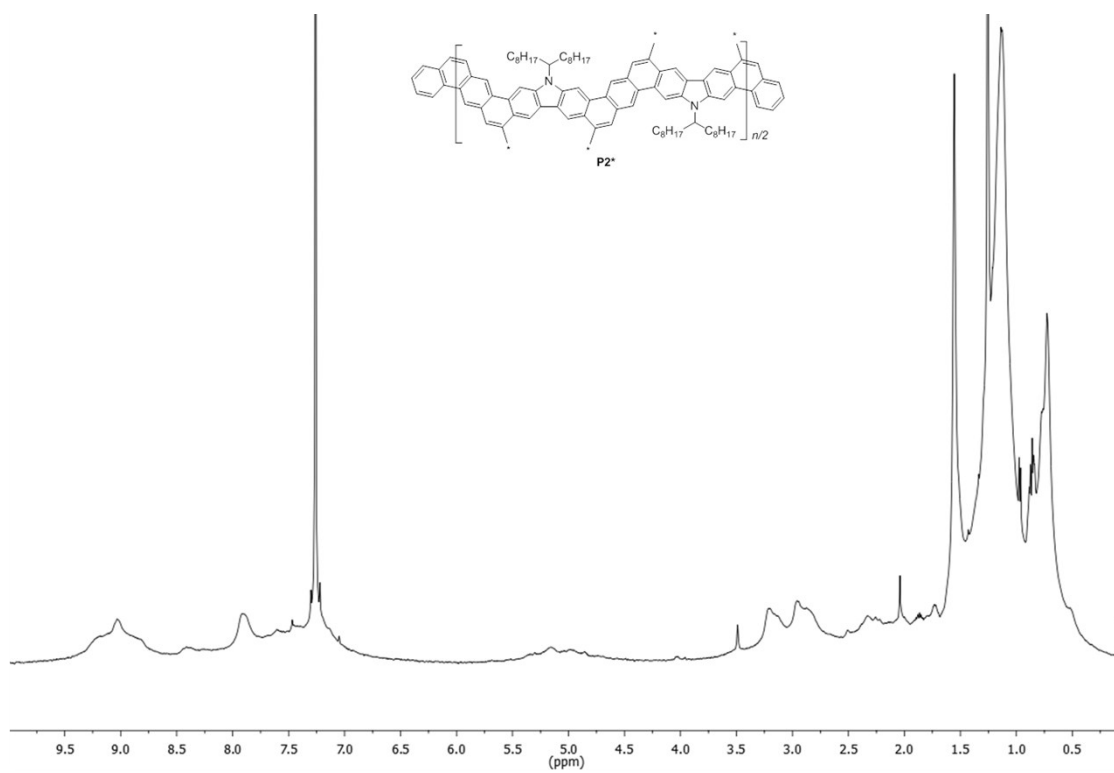


Figure S28. ^1H NMR of **P2*** (500 MHz, CDCl_3 , RT).

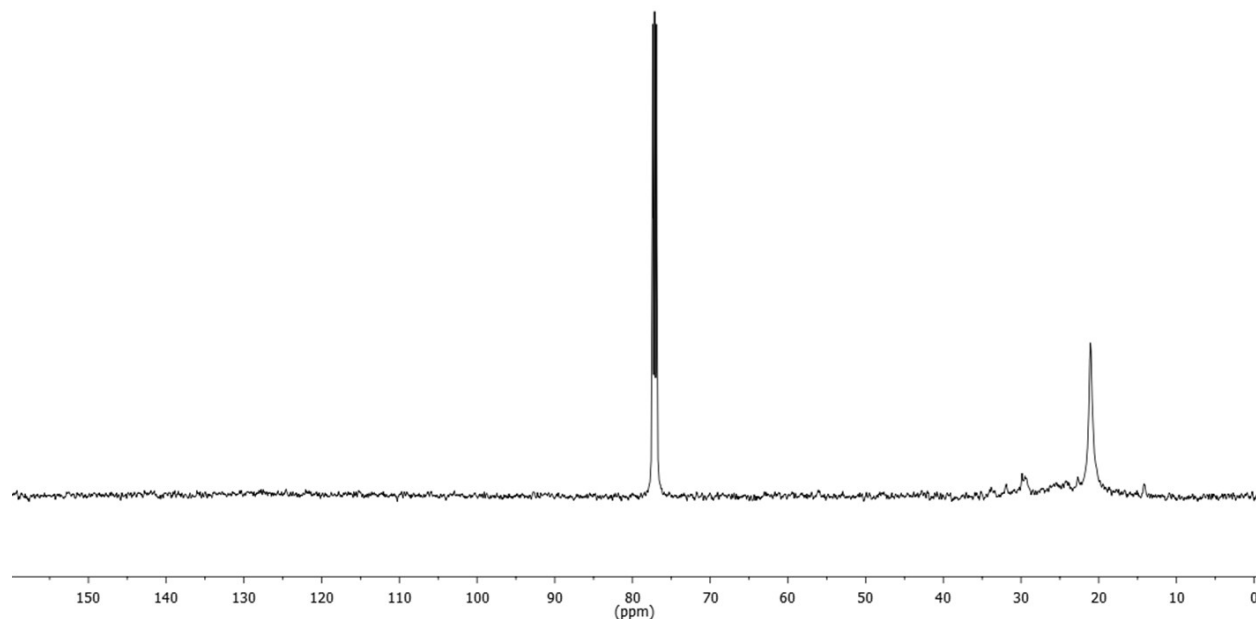
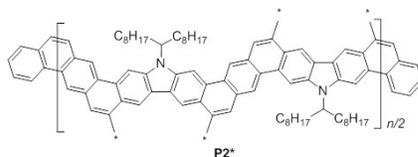


Figure S29. ¹³C NMR of **P2*** (125 MHz, CDCl₃, RT). S/N ratio of the spectrum is 376.

9. Quantum Yield

Quantum yield of **P1** and **P2** was measured by Edinburgh Instruments FLS920. 10⁻⁶ M solution of **P1** and **P2** in CHCl₃ was used to measure quantum yields by integrating sphere system using the excited wavelength 285 nm and 400 nm, respectively. Quantum yield of **P1** was too low to quantify. Quantum yield of **P2** was measured to be 15 %.

10. UV/vis and Fluorescence Spectra

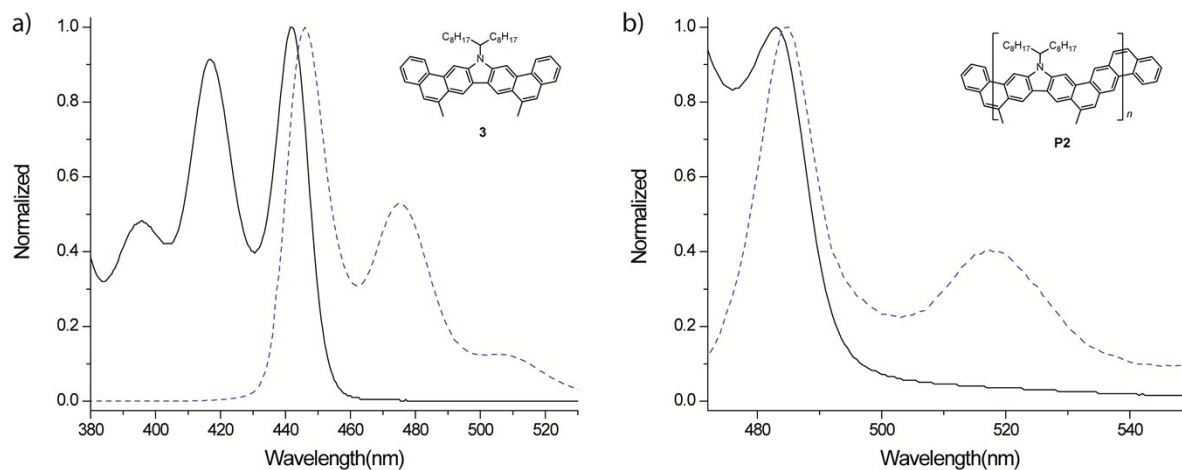


Figure S30. a) Normalized UV/vis (black solid) and fluorescence (blue dash) spectra of **3** in the range of 380-530 nm. The difference between HOMO-LUMO transition of absorption and LUMO-HOMO transition of emission of **3** was measured to be ~4 nm. b) Normalized UV/vis (black solid) and fluorescence (blue dash) spectra of **P2** in the range of 380-530 nm. The difference between HOMO-LUMO transition of absorption and LUMO-HOMO transition of emission of **P2** was measured to be ~1 nm.

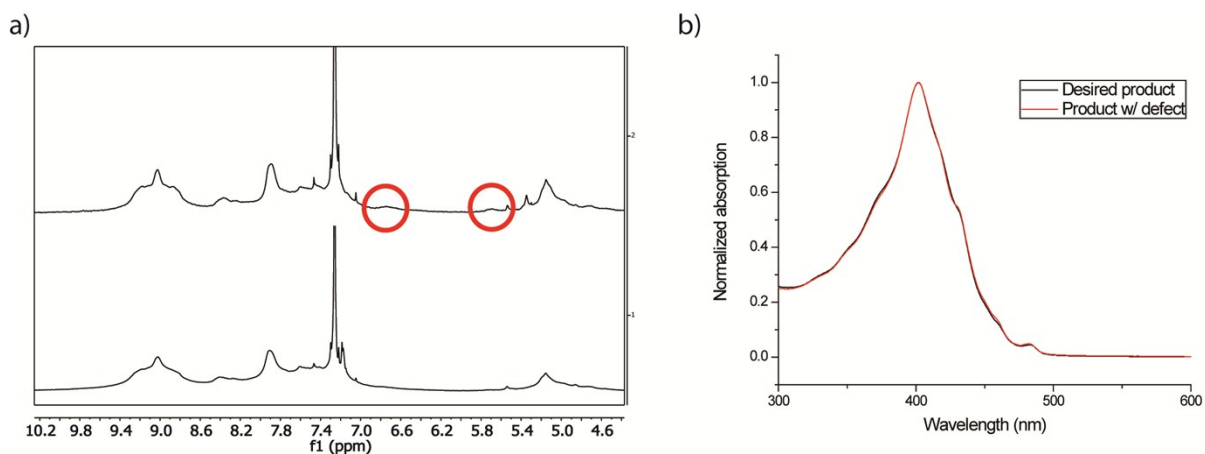


Figure S31. a) ¹H NMR of the product with small amount of defect (red circles, top) and the desired product (bottom). b) Normalized UV-vis spectrum of the product with small amount of defect (red) and the desired product (black).

11. Thermal Gravimetric Analysis (TGA)

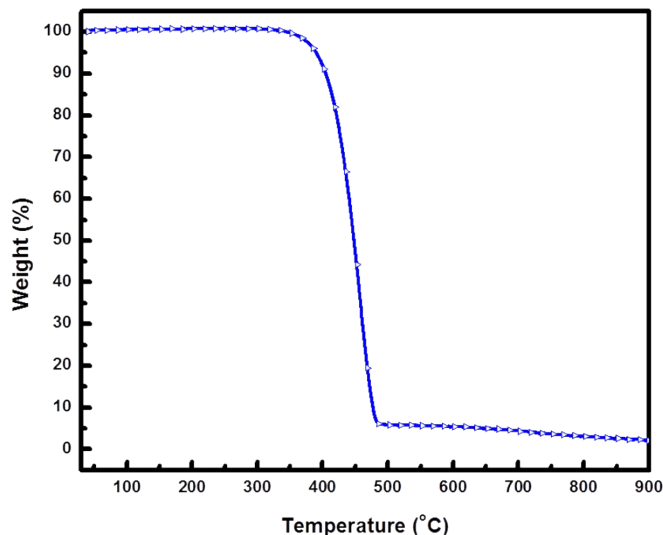


Figure S32. TGA trace of **3**. The sample lost 5 % weight at 390 °C as a result of sublimation. The full sublimation range was 450 - 485 °C.

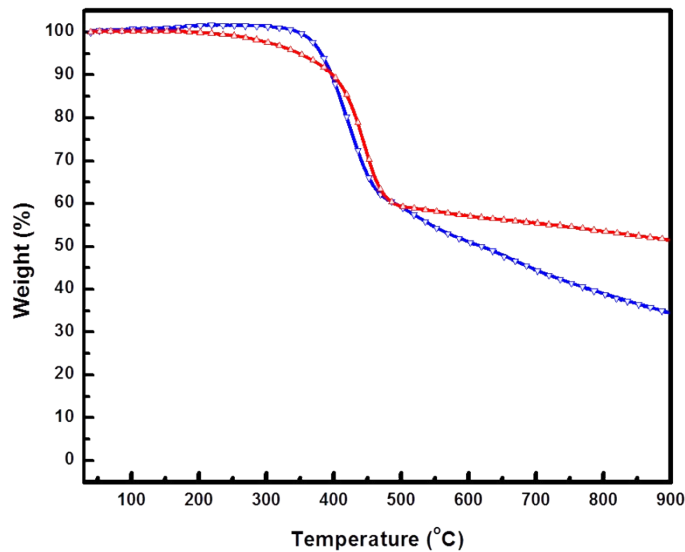


Figure S33. TGA trace of **P1** (blue) and **P2** (red). Decomposition temperature of **P1** (T_d , 5 % weight loss) was 380 °C with a 34 % carbonization yield at 900 °C. Decomposition temperature of **P2** (T_d , 5 % weight loss) is 348 °C with a 52 % carbonization yield at 900 °C.

12. Differential Scanning Calorimetry (DSC)

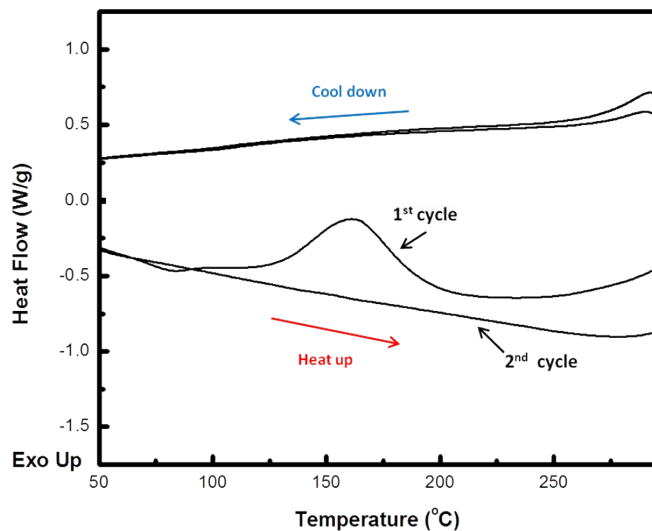


Figure S34. DSC trace of **P1**. Onset of the exothermic transition (129 °C) in the 1st cycle indicates a irreversible reaction because no transition was observed in the 2nd cycle. The sample after 2nd cycle was not soluble at all in CHCl₃. The reaction takes place at 129 °C was probably the free radical cross-linking of the vinyl groups.

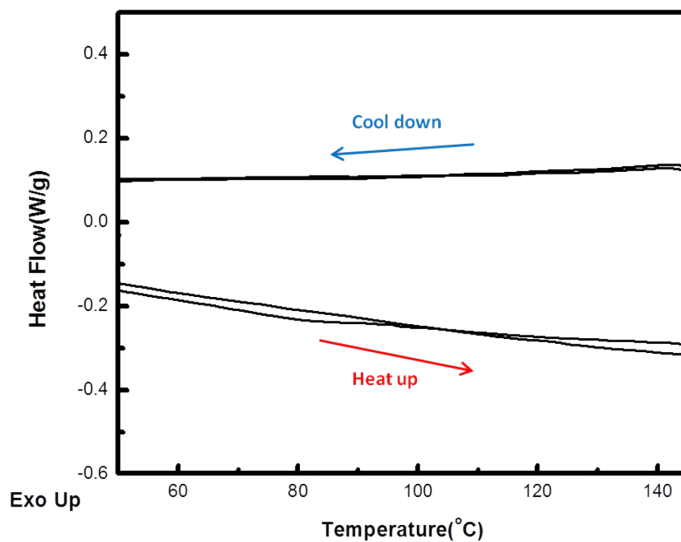


Figure S35. DSC trace of **P2**. No thermal transition or reaction was observed.

13. DFT Calculation

Atomic structures of model oligomers were optimized with density functional theory (DFT) calculations using the B3LYP/6-311G. Molecular orbital shapes and energies were calculated at the optimized geometries. The alkyl chains are replaced with isopropyl groups for computational simplicity. Orbital pictures were generated with Gaussview 5.08. For compound **3** computed electronic spectra, B3LYP/6-311G(d,p) was applied to optimize the atomic structure with DFT calculation, and UV/vis spectra was calculated with time-dependent density functional theory (TDDFT) at optimized geometries with same level. All quantum-chemical calculations were performed with the Gaussian09 package.⁷

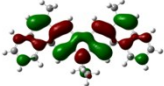
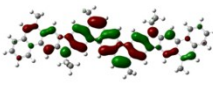
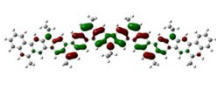
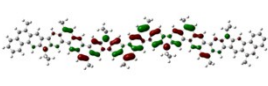
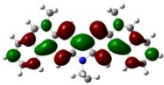
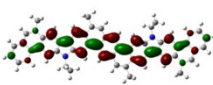
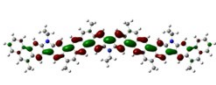
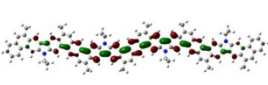
	N=1	N=2	N=3	N=4
LUMO	 -1.63eV	 -1.81eV	 -1.87eV	 -1.90eV
HOMO	 -5.20eV	 -5.03eV	 -4.99eV	 -4.97eV

Figure S36. HOMO and LUMO energy levels of model oligomer ($N=1, 2, 3$ or 4 at B3LYP/6-311G level).

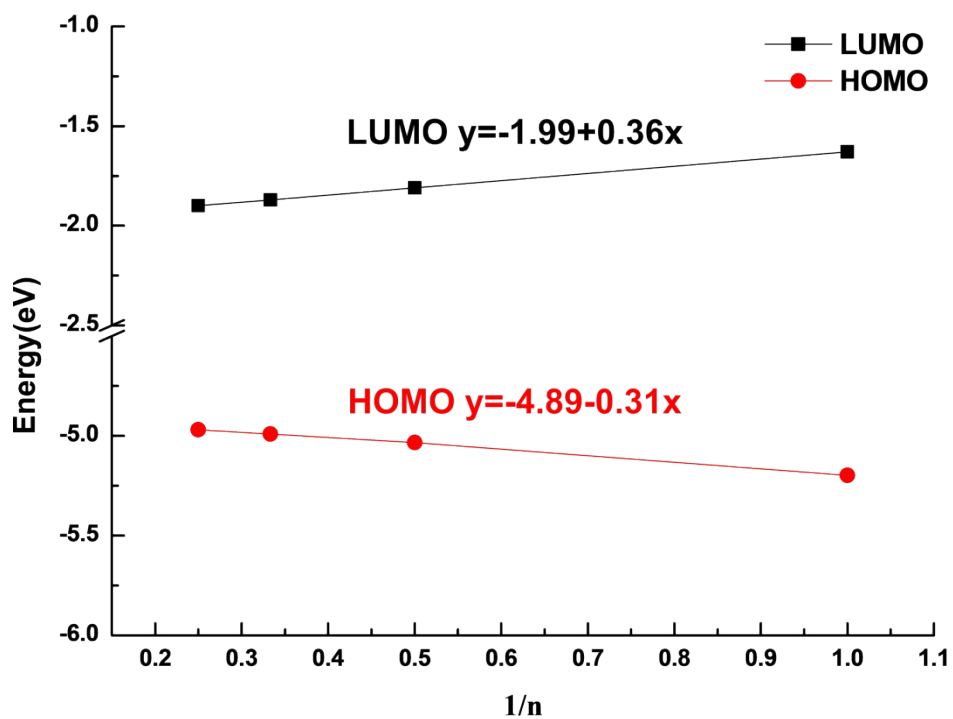


Figure S37. HOMO and LUMO energy levels for fully conjugated polymer were extrapolated from the values computed for model oligomers ($N = 1, 2, 3$ or 4 at B3LYP/6-311G level). $E_{\text{HOMO}} = -4.89$ eV, $E_{\text{LUMO}} = -1.99$ eV and $E_g = 2.90$ eV.

14. Scanning Tunneling Microscopy (STM)

Scanning tunneling microscopy (STM) measurement was performed at room temperature using Easyscan 2 system from Nanosurf Inc. A 0.5 mM solution of **P1** and **P2** (0.3 mg/ml) in chloroform was prepared with alternative sonication and waiting steps of 3 mins each for ~15 mins to completely dissolve **P1** and **P2**. Highly ordered pyrolytic graphite (HOPG) substrate was heated on a hot plate to 90 °C, and a drop of **P1** and **P2** solution was added. The substrate was allowed to cool under ambient conditions before performing the imaging under constant current mode.

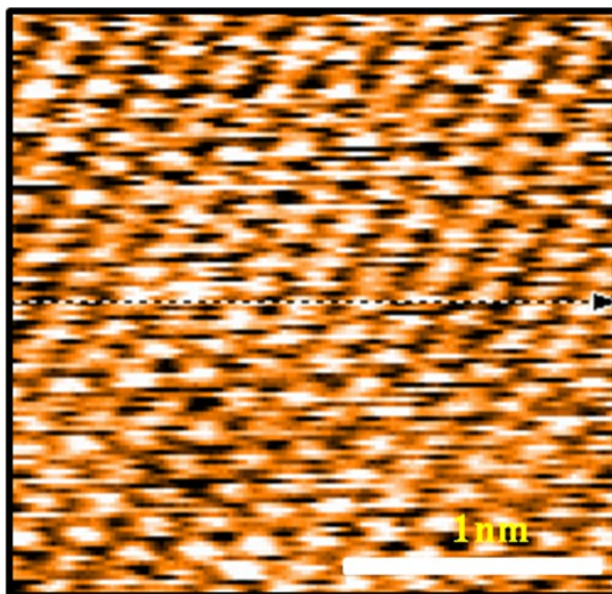


Figure S38. STM image of the bare HOPG substrate. Note that the scale bar is 1 nm, much smaller than that of the image of **P2** in the maintext.

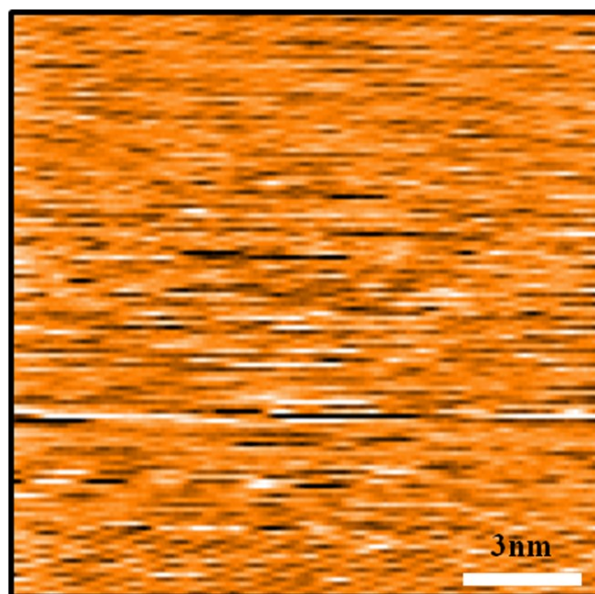


Figure S39. A representative STM image of the **P1** sample on HOPG processed under the similar condition, showing poor contact and no ordered feature. Multiple attempts have been made to identify ordered region.

15. X-ray Crystallography

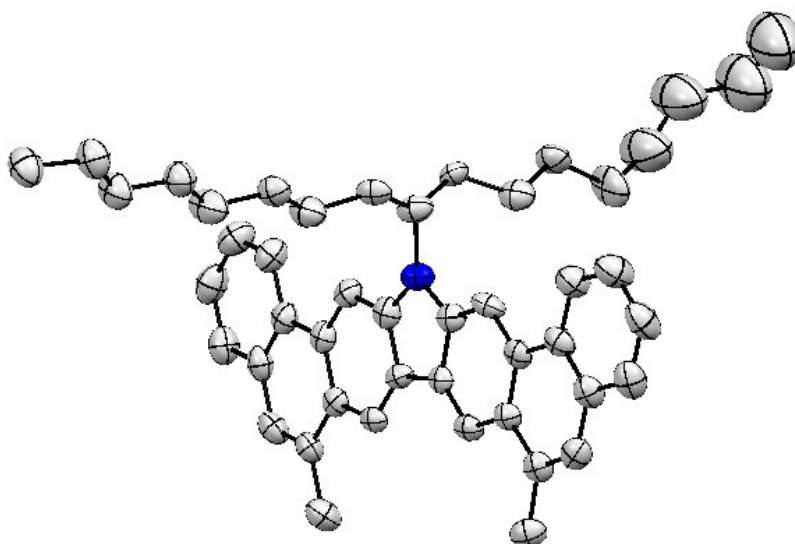


Figure S40. Single-crystal X-ray structure of **3** with probability ellipsoids set at 50% level. Hydrogen atoms have been omitted for clarity.

3: CIF file can be obtained from the supplementary information. **CCDC-1040797** contains the supplementary crystallographic data for this paper. These data can be obtained free of charge from The Cambridge Crystallographic Data Centre via www.ccdc.cam.ac.uk/data_request/cif. A yellow plate crystal of **3** having approximate dimensions of 0.435 mm x 0.195 mm x 0.056 mm was mounted on a nylon loop. Cell constants and an orientation matrix for data collection corresponded to a Triclinic cell with dimensions:

$$a = 14.501(4) \text{ \AA} \quad \square\alpha = 62.892(4)^\circ$$

$$b = 20.180(6) \text{ \AA} \quad \square\beta = 84.149(4)^\circ$$

$$c = 22.027(7) \text{ \AA} \quad \square\gamma = 77.270(4)^\circ$$

$$V = 5597(3) \text{ \AA}^3$$

For $Z = 6$ and F.W. = 633.92, the calculated density is 1.129 Mg/m³. Systematic reflection conditions and statistical tests of the data suggested the space group $P-1$. The data were collected at a temperature of 110.15 K with a theta range for the data collection of 1.039 to 20.870°.

16. Reference

1. Zhang, Z. -G.; Liu, Y.; Yang, Y.; Hou, K.; Bo, P.; Zhao, G.; Zhang, M.; Guo, X.; Kang, E.; Li, Y. *Macromolecules* **2010**, *43*, 9376.
2. Bonifacio, M. C.; Robertson, C. R.; Jung, J. -Y; King, B. T. *J. Org. Chem.* **2005**, *70*, 8522.
3. Chen, C.; Dugan T. R.; Brennessel, W. W.; Weix, D. J.; Holland, P. L. *J. Am. Chem. Soc.* **2014**, *136*, 945.
4. Jiang, Z.; Li, X. F.; Strzalka, J.; Sprung, M.; Sun, T.; Sandy, A. R.; Narayanan, S.; Lee, D. R.; Wang, J. *J. Synchrot. Radiat.* **2012**, *19*, 627-636.
5. Jiang, Z., *GIXSGUI is available for download:*

<http://www.aps.anl.gov/Sectors/Sector8/Operations/GIXSGUI.html>.

6. Hong, S. H.; Day, M. W.; Grubbs, R. H. *J. Am. Chem. Soc.* **2004**, *126*, 7414.
7. Gaussian 09 (Gaussian, Inc., Wallingford, CT, USA, 2009).